Corresponding author:
Chen Gang; Email: chengang201206@163.com

Ancient-present tectonic differences and evolution characteristics of the Meso-Neoproterozoic in the southern Ordos Basin

Li Xiaoke[1], Chen Gang[2] , Shi Jianchao[1], Song Peng[1], Liu Jian[1], Sun Dong[1] and Wang Di[1]

[1]Exploration and Development Institute of Changqing Oilfield Company, PetroChina, Xi'an, Shaanxi 710018, China and [2]State Key Laboratory of Continental Dynamics, Department of Geology, Northwest University, Xi'an 710069, China

Abstract

As international exploration of the Meso-Neoproterozoic continues, these layers have become a key target for deep oil and gas field exploration. The Ordos Basin exhibits considerable sedimentary thicknesses within the Meso-Neoproterozoic. However, significant hydrocarbon discoveries have not been forthcoming, primarily due to the complex tectonic evolution. This paper focuses on the southern Ordos Basin, utilizing logging-seismic calibration to interpret seismic data and elucidate Meso-Neoproterozoic tectonic features. By comparing ancient and modern tectonic patterns, based on palaeotectonic maps retrieved through the impression method and combining these with tectonic evolution profiles, the study clarifies the history of tectonic modification. Under the control of two fracture systems – basin-controlling fractures at the margin and trough-controlling fractures – the Changchengian exhibits two categories (single-fault and double-fault) and five sub-categories of fault depression combinations. The study highlights significant differences between ancient and modern tectonics in the Meso-Neoproterozoic, which are attributed to various tectonic stages, including the trough-uplift depositional differentiation stage during the early rift-late depression of the Changchengian, the basin-margin subsidence stage of the southwestern depression of the Jixianian, the uplift and denudation stage of the Sinian basin's main body and the four-stage tectonic remodelling stage of differential uplift-subsidence in the Palaeoproterozoic. This study employs the ancient-present tectonic pattern as a point of departure, thereby enhancing the theoretical understanding of deep-seated tectonics in the Ordos Basin. It offers novel insights into the exploration of Meso-Neoproterozoic gas reservoirs from a tectonic remodelling perspective.

CAMBRIDGE
UNIVERSITY PRESS

1. Introduction

The gradual emphasis on ultra-deep oil and gas exploration in recent years has resulted in the discovery of large Meso-Neoproterozoic gas fields in various locations, including Siberia, Arabia, Eastern Europe, Africa, Australia and India (Wang & Han, 2011). Multiple primary oil and gas fields were discovered in the Riphean and Vendian of the Meso-Neoproterozoic in the Siberian Craton (Dickas, 1986; Kuznetsov, 1997; Lottaroli *et al.* 2009; Howard *et al.* 2012). Proven recoverable reserves in Meso-Neoproterozoic siliciclastic and carbonate reservoirs are estimated to be about 600 million tonnes of oil and more than 2700 billion cubic metres of gas (Efimov *et al.* 2012). Nine Meso-Neoproterozoic carbonate reservoirs have been discovered in the Klust area, southern Oman, with proven crude oil reserves of 350 million cubic metres (Al-Riyami *et al.* 2005; O'Dell & Lamers 2005; Grosjean *et al.* 2009). The Velkerri Formation of the Proterozoic Roper Group in the McArthur Basin, northern Australia, exhibits favourable indications of oil and gas (Mukherjee & Large, 2016; Jarrett Amber *et al.* 2019). The study of Meso-Neoproterozoic gas reservoirs in China mainly focuses on the Sinian in the Sichuan Basin and the Meso-Neoproterozoic in North China (Sun *et al.* 1981; Zhao *et al.* 2023; Jiang & Cai, 2023; Yusong *et al.* 2024; Zhao, Jiang *et al.* 2024), among which the Meso-Neoproterozoic oil seedlings in the North China Craton Rift Trough are confirmed to be derived from Meso-Neoproterozoic sediments by stable carbon isotope comparisons (Wang *et al.* 2004; Wang *et al.* 2019; Wang & Han, 2011; Wu *et al.* 2016). The discovery of the Sinian Anyue mega gas field in the Sichuan Basin, with a geological reserve of more than $1*10^{12} m^3$ (Zou *et al.* 2014; Wei *et al.* 2015), provides confirmation of the potential existence of extensive oil and gas fields in the Meso-Neoproterozoic of China's large-scale Craton Superposition Basin (Sun & Xie 1980; Li, Lang *et al.* 2011; Zhao *et al.* 2018; Zhang *et al.* 2023; Yusong *et al.* 2024).

The Ordos Basin is a sedimentary basin with obvious stable subsidence, depression migration and torsion. A thick layer of Meso-Neoproterozoic is developed on the crystalline basement in the south-central part of the basin, and the Changchengian, Jixianian and Sinian are developed from

the bottom up. The recent display of Meso-Neoproterozoic natural gas in the Hangjinqi area (Peng, 2009), as well as the Changchengian hydrocarbon source rocks in the Luonan and Yongji areas (Hao et al. 2016; Zhao et al. 2018), and the discovery of solid bitumen in the Jixianian system (Li, Lang et al. 2011) all indicate that there is a significant potential for natural gas exploration in the Meso-Neoproterozoic in the southern part of the basin. Early scholars regarded the Ordos Basin as a rift valley stage from the Middle Neoproterozoic to the Early-Middle Cambrian, with the Qinling, the North Qilian and the Helan Mountains constituting the Trifurcated Rift Valley System (Tan et al. 2024; Fan, Qi et al. 2024; Zhao, 1983). It is also believed that a series of rift troughs were developed in the Middle and Lower Palaeozoic basins, such as the Ansumiao-Huanxian rift trough, the Fuxian-Jingchuan rift trough and the Rift Shoulder formed by the Early Palaeozoic rift valley reactivation (Zhu, 1987; Lin & Zhang 1995). Recently, many scholars through geophysical data research that the Ordos Massif started to deposit the first set of cover layers in the Changchengian Period of the Middle Proterozoic, and accompanied by the tensile action of the North China Massif during the same period (Li et al. 2024), a series of 'depression troughs' or 'rift troughs' were developed in the basin, including Helan, Ningmeng, Ganshan and Jinshan rift troughs (Guo et al. 2016; Zhao et al. 2018). In the rift trough, the main development of the Changchengian coastal shallow marine terrestrial clastic deposition or clastic tidal flat deposition is represented by the Gaoshanhe Group (Gao et al. 2016; Ouyang et al. 2020). During the sedimentary period of Jixianian, the tectonic environment in the basin changed into depression subsidence, and the carbonate rock deposition of shallow sea platform facies was developed (Zhao et al. 2012; Zhang 2015; Feng et al. 2018; Feng et al. 2020; Chen, Zhou et al. 2020; Wang et al. 2020). The Sinian period is characterized by the development of typical glacial sedimentary products, mainly for the Luoluan or Zhengmuguan Group moraine conglomerate (Liu et al. 2024; Cai et al. 2013; Dong, 2018; Bao et al. 2019; Bai et al. 2020; Li et al. 2023).

Palaeotopography gives rise to variations in depositional environments and sedimentary products, while the tectonic modification process exerts control over differences in hydrocarbon geological conditions. However, the current tectonic study of the Meso-Neoproterozoic is primarily concerned with the portrayal of the present tectonic pattern. The study of palaeotopography during the sedimentary period remains at the theoretical stage, and the investigation of the modification of the Meso-Neoproterozoic in the context of tectonic evolution is still in its infancy, giving rise to a multitude of controversies within the field of reservoir formation theory. In this paper, seismic data processing is employed to utilize synthetic seismic record calibration for the interpretation of seismic data within the specified study area. The present tectonic pattern of Meso-Neoproterozoic systems in the study area is elucidated, and it is proposed that five distinct fault depression system combination styles are developed in the rift trough of the Changchengian system. Using the impression method and 2DMOVE software for palaeotectonic restoration and tectonic modification history recovery, the Changchengian palaeotectonic pattern is high in the east and low in the west, with the characteristics of 'two troughs and two uplifts'; the study area was a southwest-dipping slope during the Jixianian; the main body of the Sinian basin is denuded palaeocontinent, with local depressions along the western and southern margins. This study has meticulously delineated the distinctions between ancient and modern tectonic patterns, elucidated the process of tectonic modification, augmented the

fundamental geological theories of the Meso-Neoproterozoic era and has significant guiding value for the exploration of deep-seated oil and gas in the Ordos Basin.

2. Geological setting

The Ordos Basin is a multi-cycle superposed basin formed on top of the western land mass of the North China Craton, and the study area is located in the southern part of the basin where the Neoproterozoic boundary is thickly developed, bounded by the Qingtongxia-Guyuan Fracture in the west, the Fangshan-Lishi area in the east and the Weibei Uplift Fracture in the south (Fig. 1a). The Meso-Neoproterozoic develops the Changchengian, Jixianian and Sinian from the bottom up, and the depositional extent decreases sequentially to the southwest of the study area. As the first set of sedimentary cover overlying the basement of the Palaeoproterozoic, the Meso-Neoproterozoic has undergone multiple phases of tectonic modification. In the early Miocene, under the Columbia supercontinent rifting environment, the Ordos Basin experienced the Lvliang tectonic movement, which was mainly characterized by extensional effects, resulting in the development of Intracontinental rift troughs in the Changchengian and presenting coarse clastic rock-filled sediments in the rift troughs. In the late Changchengian, the extension and rifting activities weakened and entered the depression and subsidence stage, which resulted in the deposition of widely overlying coastal phase silty clastic rocks. Therefore, the Changchengian shows a two-layer sedimentary structure with a coarse lower layer and a fine upper layer. The main body of the basin was uplifted in the Jixianian, and the southwestern depression and subsidence area was a land surface marine environment, dominated by carbonate deposition and developing various types of dolomite. The Sinian is typical glacial deposition, developing moraine conglomerate. After the Proterozoic, the basin experienced the tectonic evolution process of differential uplift-depression in the Early Palaeozoic, continental margin collision orogeny and intra-continental depression in late Palaeozoic, and continuous intra-continental depression in the Mesozoic. The Mesozoic oil-bearing system dominated by Triassic Yanchang Formation and Jurassic Yan'an Formation reservoirs, and the Palaeozoic gas-bearing system dominated by Carboniferous and Permian gas reservoirs were formed. The Meso-Neoproterozoic, as a potential third oil- and gas-bearing system, may form a primary gas-bearing reservoir with Changchengian mudstones supplying hydrocarbons and sandstones as reservoirs, or a gas-bearing system with Mesoproterozoic reservoirs (Fig. 1b).

3. Methods

3.a. Seismic interpretation based on synthetic seismogram

Due to the lack of deep drilling data in the study area, it is difficult to support the fine interpretation of the structure, and it is necessary to use the seismic data covering the whole area to supplement the research. First, the analysis of drilling core combined with logging curve is used to divide the horizon. For example, the purplish red dolomite at the bottom interface of the Cambrian in Well QS1 transits to the Changchengian clastic sandstone, and the Gamma Ray (GR) and Spontaneous Potential (SP) logging values show a high-value abrupt interface. During the transition from the Changchengian sandstone to the Palaeoproterozoic plagioclase gneiss, the GR and SP show low- and high-value mutations, respectively, thus determining the top and bottom interfaces of the
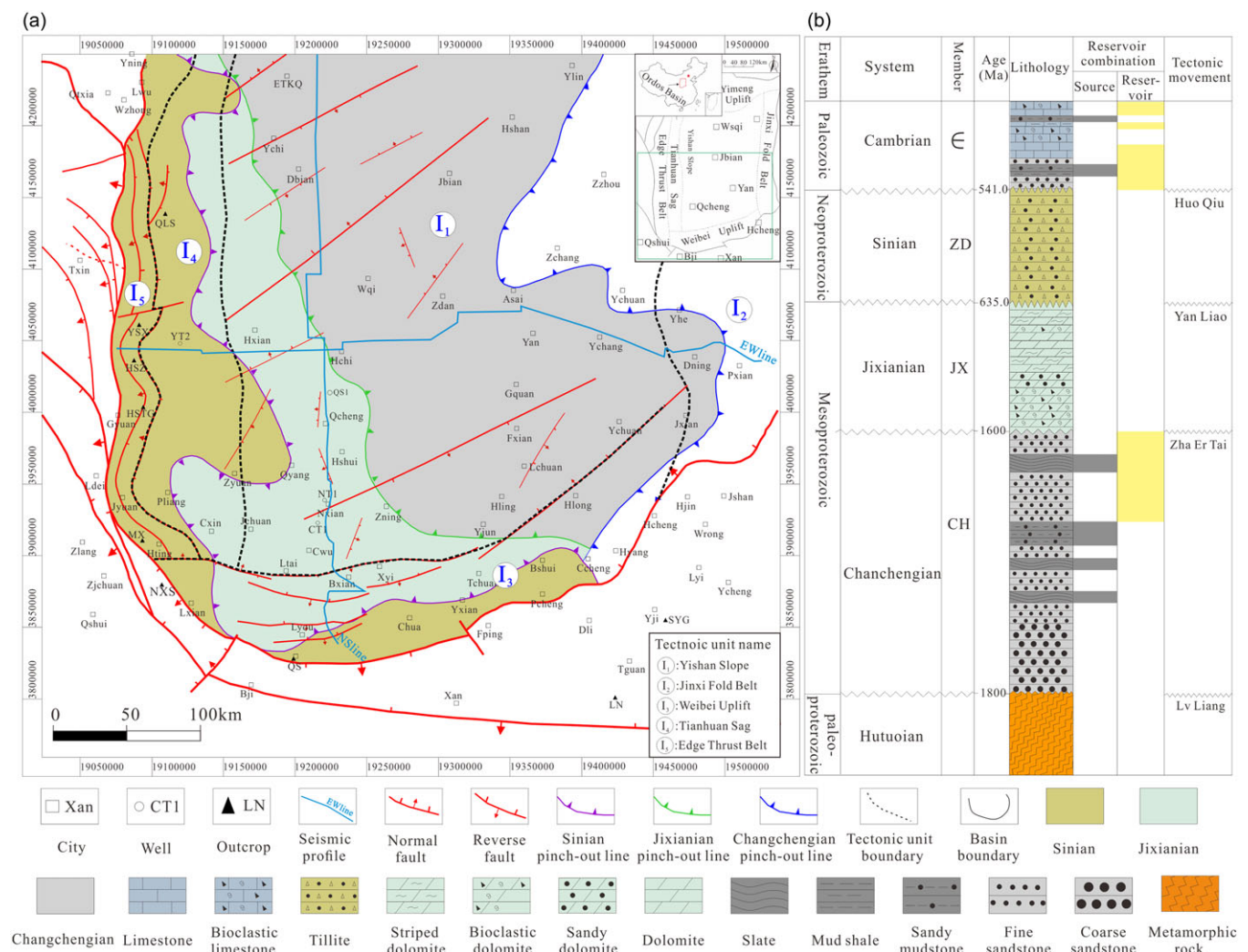
Figure 1. a. Geological map of the study area in the Ordos Basin. b. Stratigraphic histogram of the study area (the Meso-Neoproterozoic strata are divided into the Mesoproterozoic Changchengian and Jixianian and the Neoproterozoic Sinian).

Changchengian strata. Second, synthetic seismic records are produced. The synthetic seismic record is a forward process of a positive reflection coefficient and a seismic wavelet fold product. The sound velocity of each interpreted layer is determined by the inverse of the time difference of sound wave from logging, and the wave impedance and reflection coefficient of the corresponding layer are determined by its product with density; the Ricker wavelet's strict zero-phase characteristics ensure precise alignment between reflection times and stratigraphic interfaces, facilitating detailed structural interpretation, while its rapid side-lobe decay minimizes thin-layer interference effects. The seismic wavelet is determined based on the Ricker wavelet model, and the synthetic seismic record is obtained by the pleating of the reflection coefficient with the seismic wavelet. Finally, the drilling horizon is calibrated to the seismic profile by comparing the positive polarity trace in the synthetic seismic record with the original seismic profile near the well. (Seismic profiles with a 45Hz dominant frequency enhance deep-layer identification while maintaining resolution clarity; acquired with 50m trace spacing and 120-fold coverage under vibroseis source conditions).

Taking the seismic profile calibrated by Well QS1 as an example (Fig. 2), the peak of the positive synthetic record (Synthetic (+)) at the bottom interface of the Carboniferous corresponds to the wave peak at 3900m of the seismic profile; the Ordovician bottom interface corresponds to the top of the wave trough at 4000m; the wave peak at 4200m corresponds to the bottom boundary of the Cambrian system and the bottom boundary of the Changchengian is the top interface of the wave peak at 4600m (Cheng et al. 2024). By means of multi-well calibrations, the signatures of seismic reflections in each stratigraphic were determined : the grey-black mud shales at the base of the Permian demonstrate a broad-axis, strong-amplitude wave peak; while the base of the Ordovician carbonates exhibit a medium-amplitude wave trough; the bottom boundary of the Cambrian displays a medium-continuous, strong-amplitude wave peak and the lithological interface between the Changchengian and the Palaeoproterozoic metamorphic basement rock presents a medium-continuous wave peak with strong amplitude.

3.b. Balanced cross-section technique and impression method

Based on the results of seismic interpretation, the tectonic modification process of Meso-Neoproterozoic in the study area can be clarified by creating equilibrium profiles (2D Move
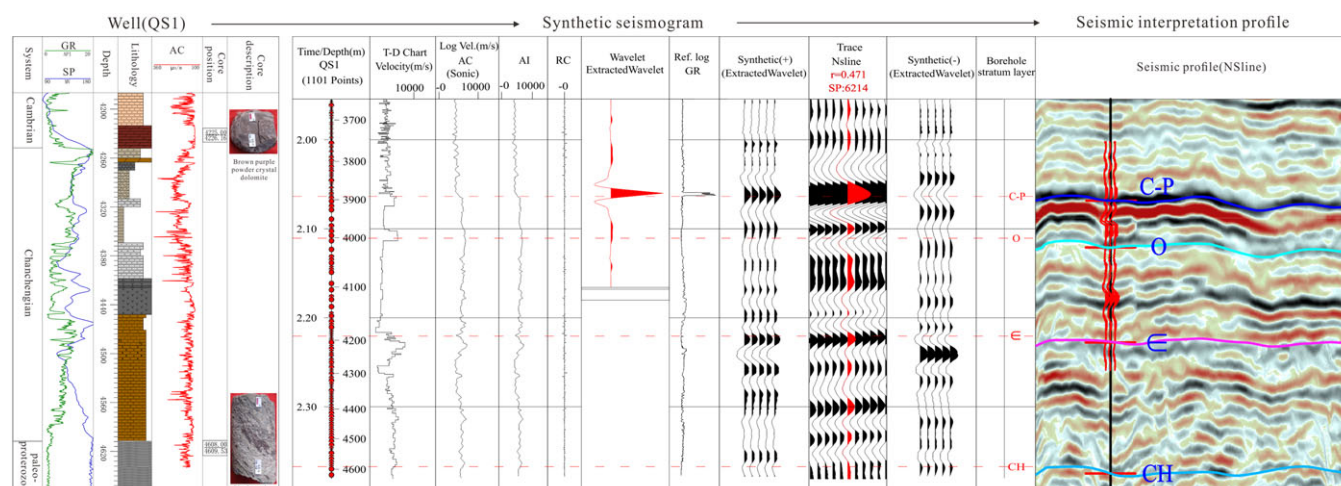
Figure 2. Synthetic seismic trace calibration and well-seismic integrated interpretation.

software) and inverting the tectonic history of different periods. The recovery of palaeotectonics by equilibrium profiles is mainly guided by the principle that the volume of the rock layers remains essentially unchanged during deformation, and the influence of regional tectonic stresses should not be neglected, in addition to the consideration of the alterations brought about by denudation and sedimentary compaction. When creating a balanced cross-section, for each period of recovery, the compaction of the overlying strata is removed first and the underlying strata will rebound upwards, the amount of rebound depending on the rock density and thickness of the overlying strata and the degree of compaction resistance of the underlying strata. The next step is to recover the faults. The faults in the study area are mostly shovel-type normal faults, which are not only longitudinally dislocated but also transversely slipped, so the fault bending and slipping algorithm is mostly used to recover the faults (Xue *et al.* 2001). Finally, the stratigraphic flattening operation is carried out, and a balanced cross-section of a geological period is completed. Repeating the above operations for each geological period, a complete tectonic evolution profile can be obtained.

At present, the common methods of ancient structure (ancient landform) restoration at home and abroad are residual thickness method, impression method, layer flattening method, compaction recovery method and so on. Due to the existence of sedimentary discontinuities between the Meso-Neoproterozoic strata in the study area, the original strata have been denuded to a certain extent, and the use of the impression method can eliminate the influence of topography before deposition and also quantitatively characterize the palaeotopography, which is very suitable for the study area. This method regards the sedimentary discontinuity as an isochronous interface when the overlying strata begin to deposit, and uses the 'mirror image' relationship between the thickness of the overlying strata and the ancient landform to quantitatively restore the shape of the ancient structure (Fig. 3). Specifically, when recovering the ancient structure of the target strata, the top boundary of the overlying strata is selected as the datum and the datum is flattened; then, the thickness from the datum to the top boundary of the target strata in the seismic interpretation profile is measured, and transformed into a planar thickness contour map (Fig. 3a) and finally, the thickness map is mirrored and flipped, to obtain the ancient terrain of the target strata (Fig. 3b).
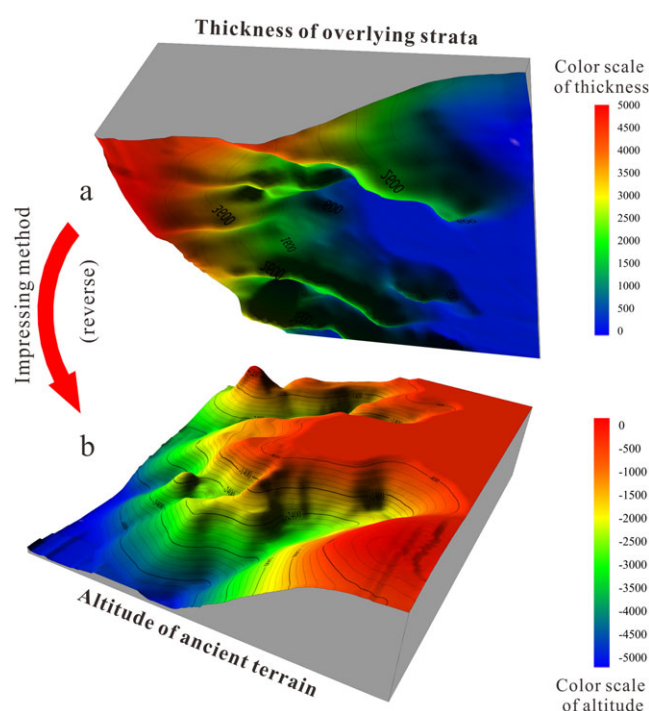

Figure 3. The example diagram of restoring palaeostructure using the impression method (Changchengian of the study area).

4. Result

4.a. Analysis of structural characteristic

4.a.1. Structural interpretation of a typical seismic section

The Meso-Neoproterozoic is a west-to-east uplifted slope in the east-west profile. The Changchengian is centred on the Qingcheng-Yulin uplift in the Hchi-Yan section, with the Ganshan rift trough and the Jinshan rift trough developing on the east and west sides (Fig. 4a). In the section to the west of Huachi, the Changchengian fault depression layer is faulted by the west-dipping Hchi-Jbian fault, which is a west-dipping and deepening stepped fault depression deposition. A fault-concave under the control of the east-dipping positive fault at the well YT2 and the Changchengian fault depression layer on the west side of
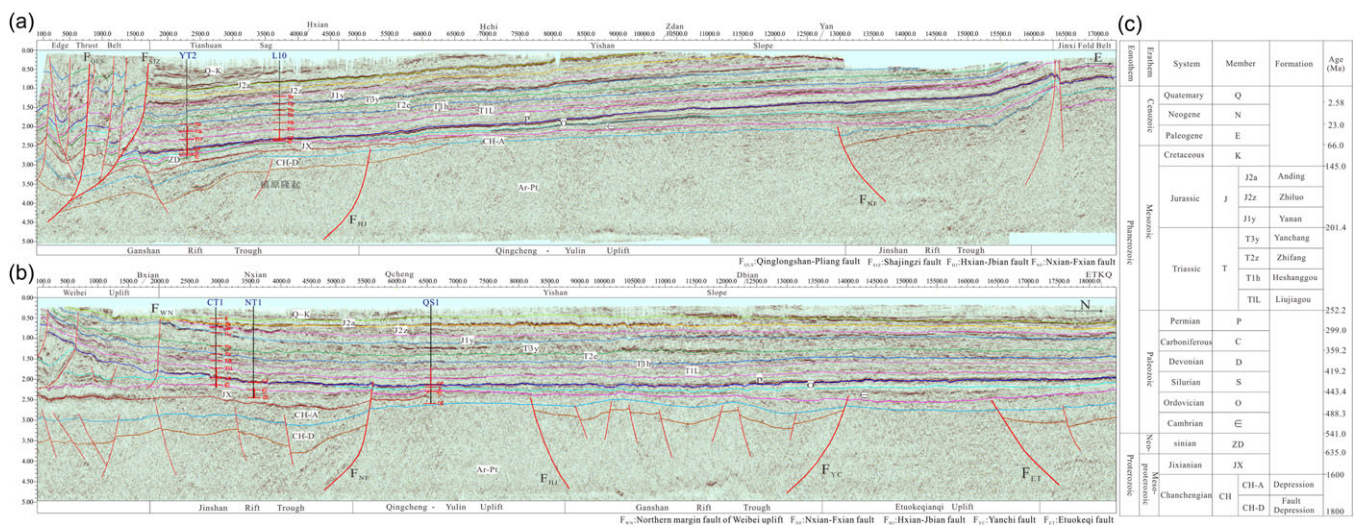
Figure 4. Comprehensive interpretation results of seismic section. a. east-west seismic profile (EWline). b. north-south seismic profile (NSline). c. stratigraphic annotation interpretation map in seismic profile.

the well are truncated by the west-edge retrograde zone at the lower plate of the Shajingzi fault, showing an anticline structure. The fault depression layer of the Changchengian in the Qingcheng-Yulin uplift to the east of Hchi is absent, and in the Jinshan rift trough, which is controlled by the Nxian-Fxian fault on the east side of the uplift, the Changchengian manifests as an eastward uplifted half-graben-like rift. The depression layer of the Changchengian is controlled by the early fault depression layer and is thickened in the Ganshan rift trough and the Jinshan rift trough, while in the Qingcheng-Yulin uplift section between the rifts, the depression layer was deposited stably with a smaller thickness. The Jixianian thins gradually from west to east and is in clipped unconformity contact with the Cambrian. To the west of well L10, the Jixianian deepens downward at the Changchengian rift groove and rises upward in the lower plate of the western rim fracture zone. The scale of Sinian deposition shrinks to the west, and the thickness is thinner than that of Jixianian, and the thickness gradually thins in the western part of Tianhuan Sag and is cut off by the overlying Cambrian strata.

In the north-south section, the Changchengian develops the Ganshan and the Jinshan rift trough, which present a tectonic pattern of 'two troughs and two uplifts' with the Etuokeqianqi and the Qingcheng-Yulin uplift on both sides (Fig. 4b). The secondary faults in the Jinshan rift trough in the section south of Qcheng are developed, and the Changchengian fault depression layer is a block-type deposition thickened to the south, while the fault depression layer in the Weibei uplift area is faulted by a step-like normal fault and uplifted to the south. The Ganshan rift trough in the middle of the profile is controlled by the positive faults on both sides, and the fault depression layer is in the form of a 'Graben-horst composite rift' by secondary faults. Besides, the Changchengian only develops depression layer in the Qingcheng-Yulin uplift and Etuokeqianqi uplift area, the depression layer is affected by the undulation of the bottom fault depression topography, and the overall thickness is thickened in the fault depression or thinned out in the uplift. The Jixianian is developed in the section south of the QS1 well, successively thickened in the Jinshan rift trough, uplifted and thinned in the Weibei uplift and is in a clipped unconformity contact with the overlying Cambrian.

4.a.2. The fault system of Meso-Neoproterozoic

The Meso-Neoproterozoic fracture system is divided into two types: basin-controlling fractures at the basin margin and trough-controlling fractures within the basin (Fig. 5). Among the basin-controlling rupture combinations at the western edge of the basin, the Qingtongxia-Guyuan fault (F_{QTX}) separates the Ordos Basin and the Qilian orogenic belt and forms a north-south trending west-trending reversed fault combination with the Qingshongshan-Pingliang (F_{QLS}), Huianbao (F_{HAB}) and the Shajingzi fault (F_{SJZ}). This set of reverse faults had not been formed before the Early Palaeozoic and had no influence on the rift valley in the basin and the stable land margin deposition in the later stage (Zhang et al. 2008). In the Late Palaeozoic, the extrusion tectonic stresses on the western margin of the basin took shape under the influence of the west-to-east extrusion stresses of the Qilian orogenic belt. Since the Mesozoic, under the influence of the Indo-Chinese movement, this fracture assemblage cut through the metamorphic crystalline basement and continued to retrograde to the east (Bao et al. 2019; Chen et al. 2020; Chen et al. 2024). The original westward deepening pattern of the Meso-Neoproterozoic was modified, and together with the Palaeozoic, an eastward uplifted retrograde thrust tectonics was formed (Yang & Zhang, 1990; Xu et al. 2019; Li, 2019).

The Lnan-Lchuan fault (F_{LLF}) in the southern part of the basin has been formed in the Meso-Neoproterozoic and presents a south-dipping tensional normal fault. In this tensional environment of the land margin rift, the Changchengian along Lnan-Lchuan shows southward deepening rift basin deposition (Peng, 2009; Feng et al. 2013; Chen et al. 2020). In the Palaeozoic, with the subduction and extinction of the Qinling Ocean, the fault belts at the southern margin of the basin were transformed into a thrust nappe structure, and the Meso-Neoproterozoic to the north of the original fault belts was modified and uplifted by the uplift of the North Qinling orogenic belt (Lu, 2009; Ren et al. 2016). The southern margin fault of the Weibei uplift (F_{WS}) is a high-angle positive fault that controls the Weibei uplift and the Weihe Graben and is mostly shaped after the reversal of the original Mesozoic reverse faults, with a long history of activity. The northern margin fault of the Weibei uplift (F_{WN}) is a fault that separates the sedimentary stability zone in the basin from the uplifted and
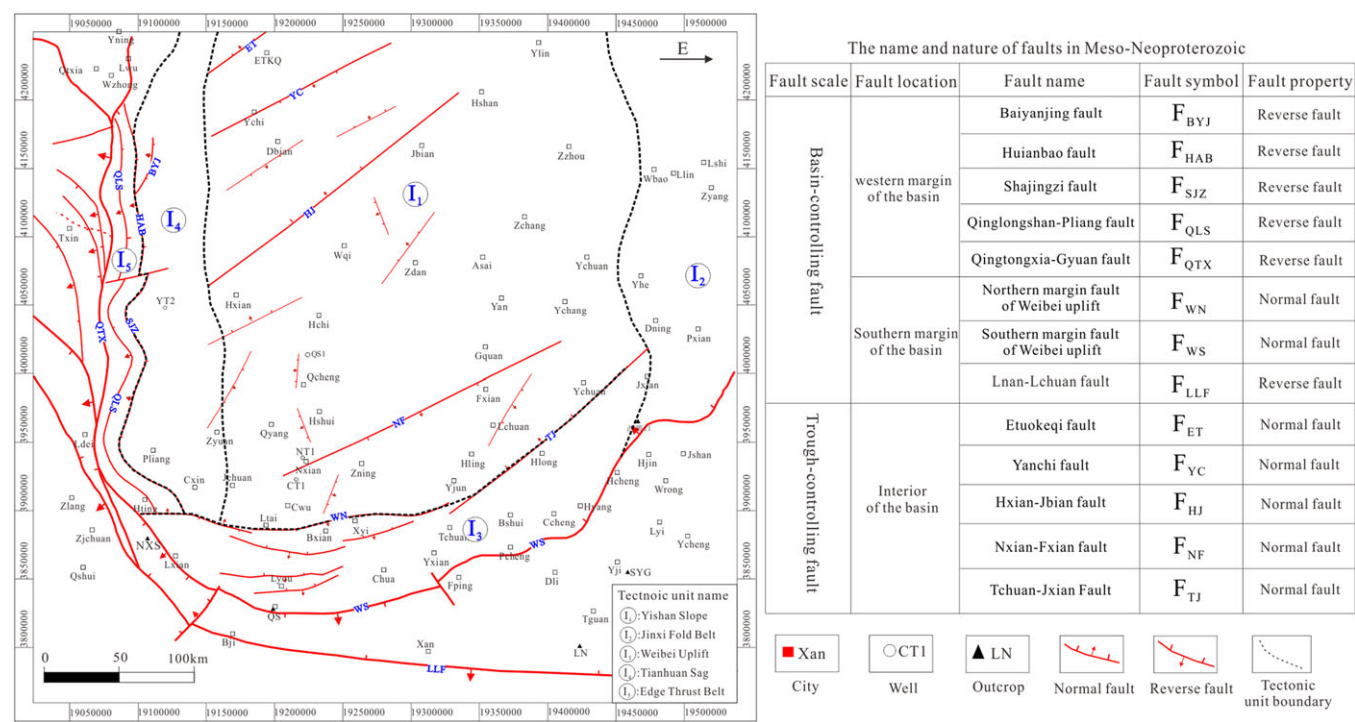
Figure 5. The fault system and distribution characteristics of the study area.

denuded zone of the Weibei uplift, and the Meso-Neoproterozoic to the south of the fault has been uplifted along with tectonic activities (Wang *et al.* 2010; Ren *et al.* 2014; Wang, Ren *et al.* 2019).

Most of the trough-controlling faults in the basin are shovel-type normal faults in the northeast direction, controlling the tectonic pattern of 'two troughs and two rises' in the study area. After the merging of the Ordos block and the North China old land in the Lvliang Movement, the rifts were formed at the basin margins under the effect of tension and the rift at the basin margins extended to the basin interior to form the sub-branching rift troughs, which formed Changchengian rift troughs controlled by the Yanci fault (F_{YC}), Hxian-Jbian fault (F_{HJ}), Nxian-Fxian fault (F_{NF}) and so on. In the middle and late Changchengian periods, these fault activities weakened, the rift troughs were no longer deepened, and the extensively developed Changchengian depression layer unconformities overlie the original rift troughs and uplifts.

4.a.3. Types and distribution characteristics of structural assemblages

Based on the geological and tectonic interpretation of the seismic profiles in the basin, the fault depression layers in the Changchengian rift trough can be classified into two major tectonic combinations, single-fault and double-fault, according to the combination of the boundary faults and the internal secondary faults (Fig. 6). The single-fault structural combination can be subdivided into half-graben-like rift and block-like rift. The half-graben-like rift is controlled by the main control fault on one side of the rift trough, and the combination with the secondary faults with different dip directions in the rift trough presents various half-graben-like rift, such as 'slope-break' and 'faulted-block' half-graben-like rift. Among them, the slope-break half-graben-like rift in the Jinshan rift trough east of Yan city, the east side of the boundary fault is the deepest part of the rift, and the slope adjacent to the rift is uplifted, constituting the slope-break half-graben-like

rift deposition combining the half-graben-like rift and the slope; another type of faulted-block half-graben-like rift in the Jinshan Rift Trough east of Zning, the combination of the boundary faults in the rift trough and the secondary faults with the opposite dip makes the Changchengian in the east side of the boundary faults in a half-graben-like filling, and under the influence of the secondary faults, the formation of upward fault blocks by step. In addition, the 'stepped' block-like rift is also an important type of single-fault rift trough, and a series of step-like normal faults divide the Changchengian into blocks in the southwestern depression area, and deepen step by step towards the southwest of the basin, forming a step-like block fault structure.

The Ganshan rift trough in the study area exhibits a double-fault structural combination, which is divided into two types due to the different combinations of internal secondary faults. The first is the graben-like rift, which is most typical of the northern part of Hxian city in the Ganshan rift trough, where the secondary faults in the rift trough are combined with the boundary faults on both sides to form a graben-like trough deposition that deepens step by step towards the centre of the rift trough. The second type is more complex. Between the boundary faults on either side of the rift trough, secondary faults with different dips and separations develop, resulting in secondary convex and concave in the rift trough, forming a 'graben-horst' composite rift, with the Changchengian deepening in the rift trough and the fault uplift on the outer side of the boundary faults.

The single-fault rift trough is widely developed in the Jinshan rift trough in the south-eastern part of the study area, and the Changchengian fault depression layer is controlled by the Nxian-Fxian fault, which shows the sedimentary structure of the north faulting and south overlapping. Among them, the slope-break half-graben-like rift is distributed in the northeast of the rift trough, and the middle-west shows the structure of a faulted block half-graben-like rift. The southwestern depression area of the thickly deposited
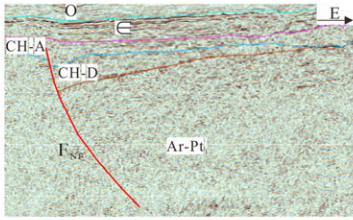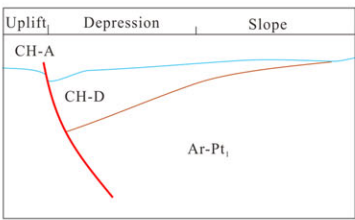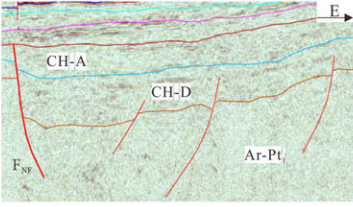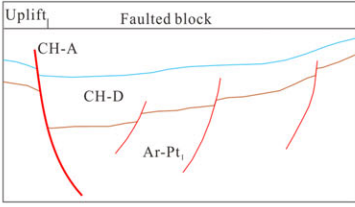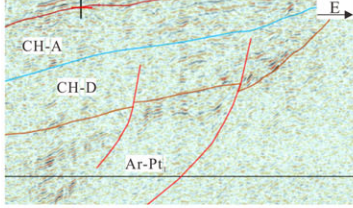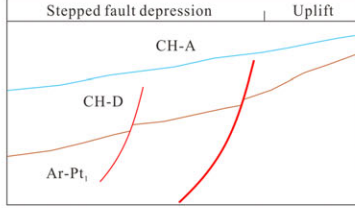
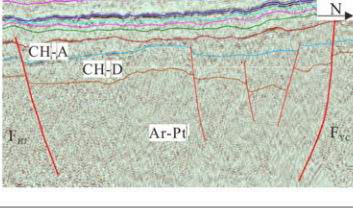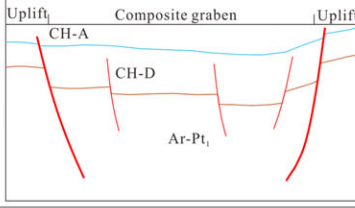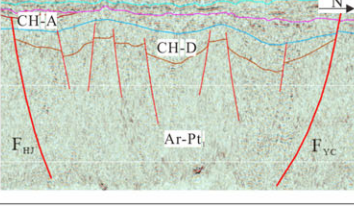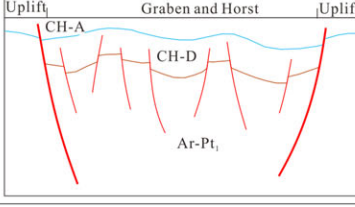| structural assemblages		Seismic Profile	structural characteristics	Development area and sedimentary characteristics
The rift trough controlled by a single major fault	"Slope-break" halfgraben-like rift	(seismic profile)	Uplift / Depression / Slope; CH-A, CH-D, Ar-Pt$_1$	Jinshan Rift Trough (East of the Yan city) — Northwest faulting and southeast overlapping
	"Faulted block" halfgraben-like rift	(seismic profile)	Uplift / Faulted block; CH-A, CH-D, Ar-Pt$_1$	Jinshan Rift Trough (East of the Zning city) — Northwest faulting and southeast overlapping
	"Stepped" block-like rift	(seismic profile)	Stepped fault depression / Uplift; CH-A, CH-D, Ar-Pt$_1$	Southwestern depression area (West of the Qcheng city) — Gradually thickened from east to west
The rift trough controlled by double faults	Graben-like rift	(seismic profile)	Uplift / Composite graben / Uplift; CH-A, CH-D, Ar-Pt$_1$	Ganshan Rift Trough (North of the Hxian city) — Asymmetric deposition on the north and south sides
	Graben-horst composite rift	(seismic profile)	Uplift / Graben and Horst / Uplift; CH-A, CH-D, Ar-Pt$_1$	Ganshan Rift Trough (South of the Dbian city) — Approximately symmetrical deposition on the north and south sides

Figure 6. Types of rift tectonic combinations of the Changchengian (Single-fault controlled trough and double-fault controlled trough can be divided into five types according to the characteristics of internal secondary fault combination).

Changchengian is influenced by stepped normal faults, and the Changchengian has a stepped block-like rift that deepens to the southwest. The Ganshan rift trough is a type of double-fault rift trough, controlled by the Yanchi and Huanxian-Jingbian faults on both sides of the trough, and combined with the secondary faults, the Changchengian fault depression layer in the eastern part of the trough is represented as a graben-like rift, while in the western part of the trough it is represented as a graben-horst composite rift (Fig. 7).

4.b. The difference of ancient-present tectonic framework

4.b.1. Ancient tectonic framework of the sedimentary period

With the breakup of the Columbia supercontinent at 1.8 Ga, its far-field extensional stresses reactivated the weak zones formed during the late Palaeoproterozoic in the Ordos Basin. Mantle upwelling or plume activities triggered lithospheric thinning and rifting, causing the formation of a series of rift troughs along the basin margins and within its interior (Liu *et al.* 2021; Zhang *et al.* 2012). During the early period of Changchengian deposition, the topography of the study area showed the characteristics of east-high and west-low, and the tectonic undulation was controlled by the 'two troughs and two uplifts' in the northeastern direction of the basin (Fig. 8). Among them, the area to the east of Zchang-Ychuan was denudation mountain during the sedimentary period, and the southwestern depression area by the Qilian-Qinling Trough cracking influence for the lower location of the structure, the Changchengian sedimentary thickness of up to 5,000m above the maximum. The central part of the study area shows a topographic pattern of alternating troughs and uplifts. The Ganshan rift trough in the north extends from Dbian to the eastern part of the basin, and there is a branching of the secondary rift trough around Hshan, which is topographically different from the Etuokeqianqi uplift and the Qincheng-Yulin uplift on both sides. The Ganshan
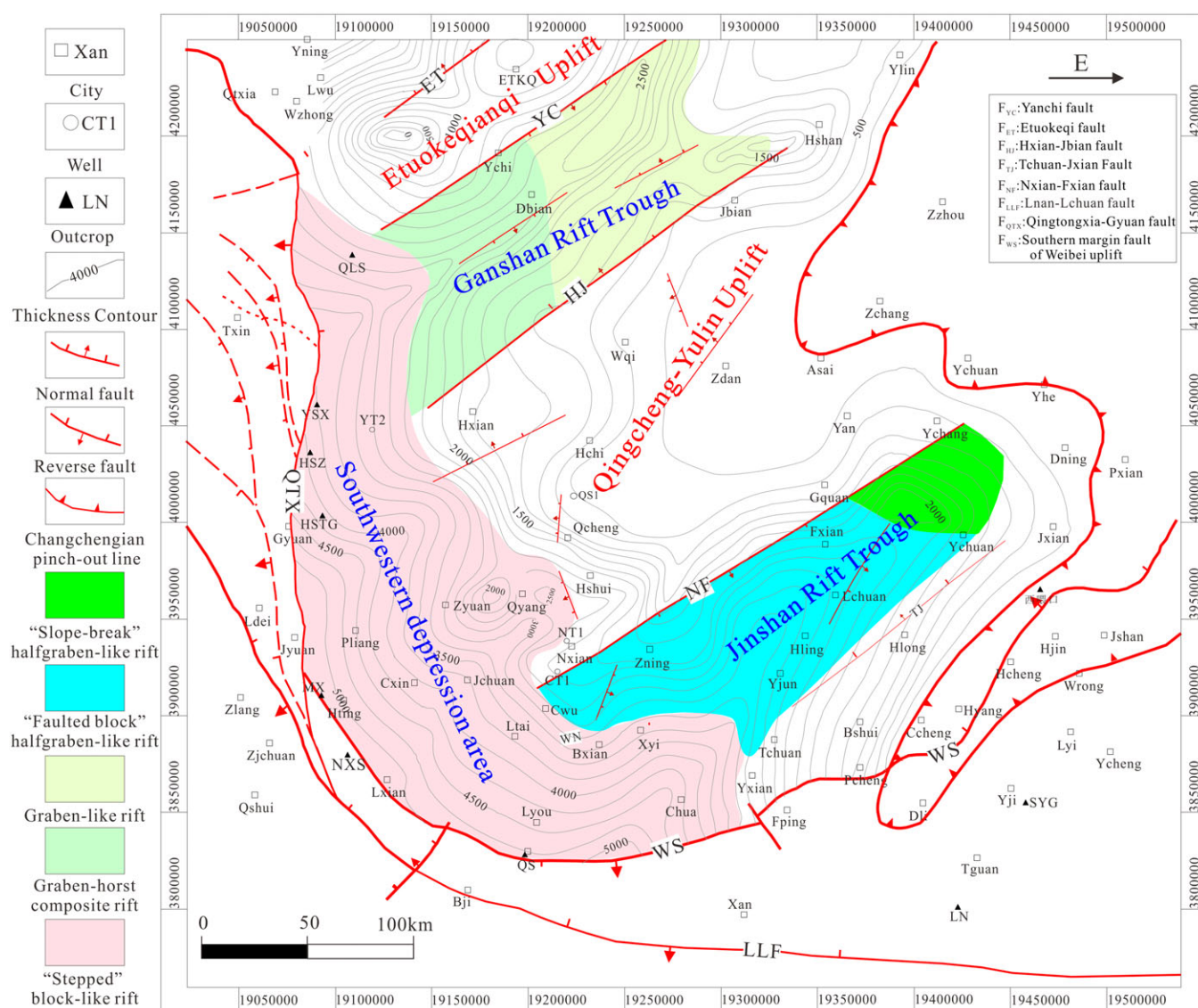
Figure 7. Plane distribution map of the Changchengian rift combination type.

rift trough in the south is wider, with the deepest rift trough in the Bxian-Chua area, and extends to the west of Yichuan, where the rift trough gradually pinches out. The early rift trough of the Changchengian was filled with sedimentary fault depression layers, and the widely distributed depression layers in the later period were not integrated to cover the fault depression layers and thickened successively in the area of the rift trough, with an overall trend of gradual thickening to the southwest.

During the Jixianian Period, the palaeotectonic framework underwent significant changes compared to the Changchengian Period. Rifting notably waned or ceased, and thermal subsidence of the basement became the dominant process within the basin (Zhang *et al.* 2018). Consequently, the basin developed an inclined slope structure deepening southwestward (Fig. 9a). As a result, the Jixianian is missing in the eastern part and is deposited in the southwestern slope area, and the thickness increases uniformly towards the southwest. The remaining thickness of the Jixianian is extinguished from north to south in the Dbian-Hchi and Yjun-Hyang areas, which are the boundaries of the Jixianian in the central-eastern part of the wide missing area, and the Jixianian is

further thickened in the southwestern part of the study area to the Pliang-Lyou area, and there is a small topographic uplift in the Bxian-Nxian area, which represents a banded area of relatively thin thickness. The absence of the Jixianian in the northwestern areas of the ZT2 and ZT1 wells may be related to the uplift and denudation of the Jixianian.

When the Sinian was deposited, the main body of the basin was a denudation mountain, and the western and southern margins had the characteristics of a basin-margin depression (Fig. 9b). Due to this palaeotectonic pattern, the Sinian is absent in the eastern part of the study area, and only deposited in the west and south side of the depression (Bai *et al.* 2022), with the thickness overall thin and thickening towards the basin margin, presenting the 'L' type spreading characteristics. In the southern depression area around Lyou-Tchuan-Bshui, the thickness of the Sinian gradually increases towards Chua-Pcheng, with a maximum thickness of 100 metres. The topography of the western depression area gradually deepens to the west, and the Sinian shows several thickness centres on the east side of the Qingtongxia-Guyuan fault, with a maximum thickness of about 150 metres.
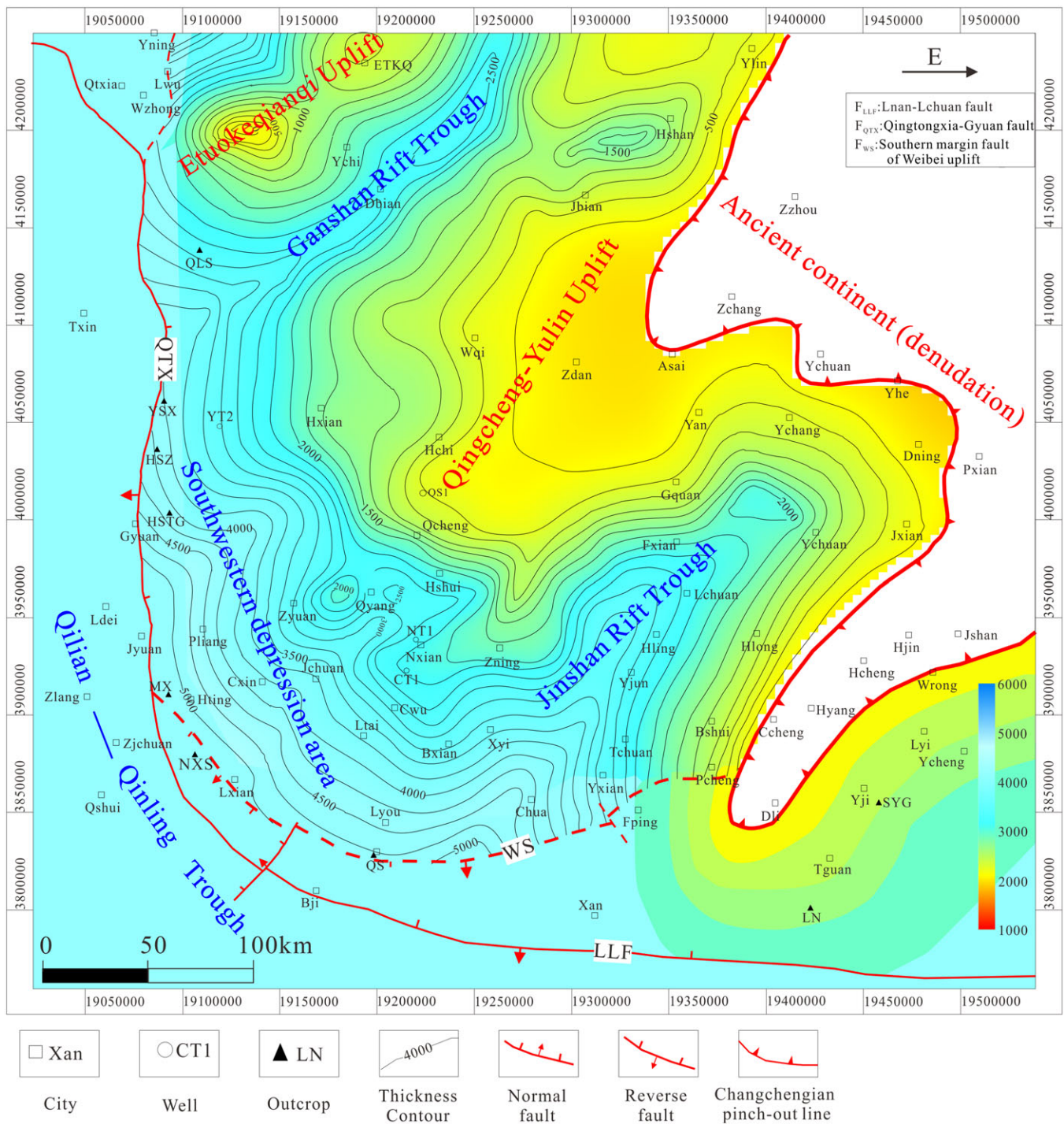
Figure 8. The ancient tectonic framework of the Changchengian (two rift troughs and two uplifts).

4.b.2. Characteristics of present planar structure

The present top surface of the Changchengian shows a southwest-trending monoclinic tectonic feature within the Yishan Slope (Fig. 10). The area south of the Nxian-Fxian fault is affected by the uplift of the Weibei uplift, showing a monoclinic pattern of deepening from east to west. The surface of the Bxian-Cwu area shows a northwest-trending nose-like structure, the root of the nose-like structure is controlled by a northeast-trending positive fault and the tectonic amplitude of the nose-like structure gradually decreases towards the west. In the northeastern Jbian-Hshan area,

the upper surface of the Changchengian shows a slope that deepens to the southwest. The Changchengian in the Weibei uplift is high in the east and low in the west, in which there are some bulges in the central part of the Weibei uplift. The area around Lyou-Bxian in the west is obviously modified by faults, and the upper surface of the area around Bshui-Hlong in the east has a higher amplitude of uplift. The Tianhuan sag is a tectonic low part of the basin; the whole is high in the north and low in the south of the tectonic features, and the development of north-south bead-shaped anticlines, the scale from north to south gradually decreases. The upper surface of the
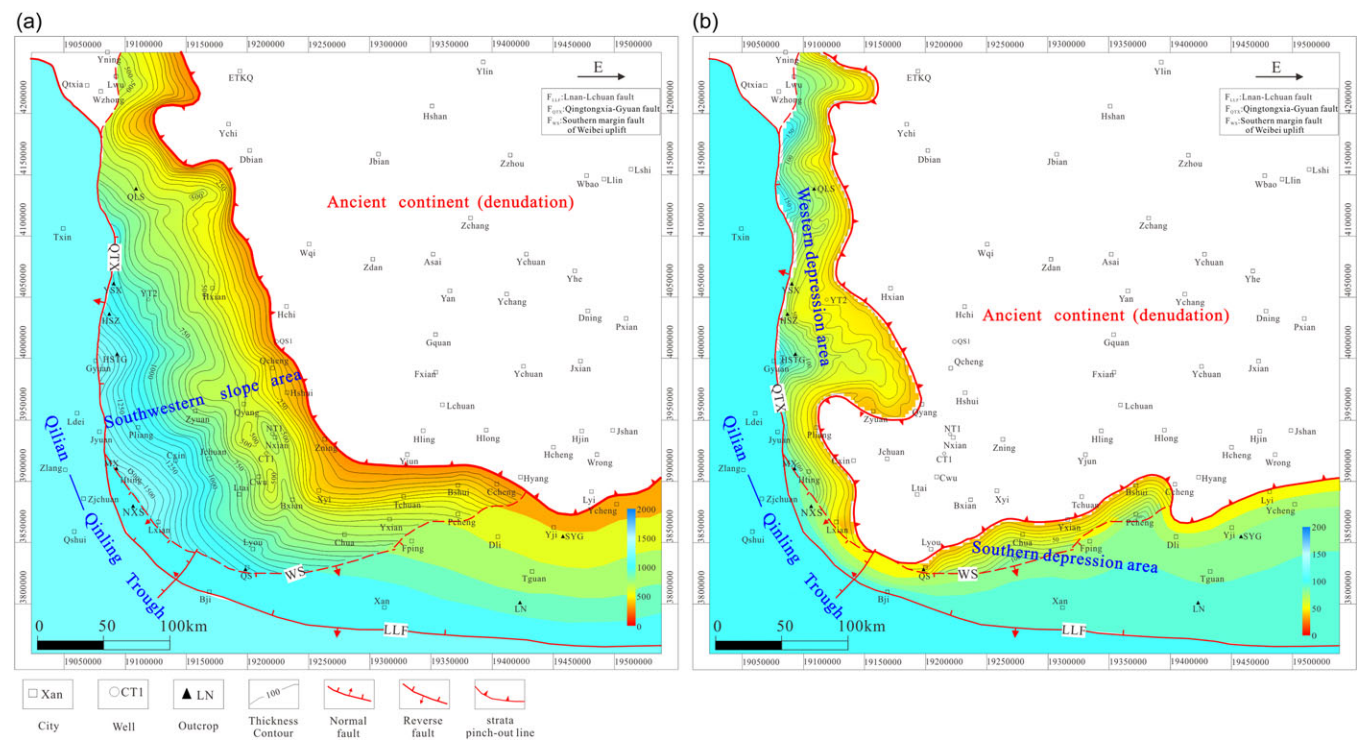
Figure 9. a. The ancient tectonic framework of the Jixianian. b. The ancient tectonic framework of the Sinian.

Changchengian within the Edge thrust belt is high in the north and low in the south, and has been altered and uplifted by north-south trending retrograde faults.

The Jixianian's top surface structure is high in the north and south and low in the centre. Among them, the internal Weibei uplift inherited the east-high and west-low character of the top surface of the Changchengian. The nose-like structure in the southwestern part of the Yishang slope is still developed, but the amplitude is smaller than that of the Changchengian, and it extends farther to the west. In the Tianhuan sag, the Jixianian is characterized by a high elevation in the north and a low elevation in the south. The north-south oriented bead-shaped anticline exhibits morphology consistent with that observed in the Changchengian. The top surface of the Jixianian in the Edge thrust belt is high in the north and low in the south, which is obviously modified by the retrograde faults, and has a great difference in height with the Jixianian in the Tianhuan sag on the east side of the Huianbao-Shajingzi Fault (Fig. 11a). The Sinian top tectonics, on the other hand, shows the characteristic of high basin periphery and low interior, which is closely related to the later basin peripheral modification and uplift. The Edge thrust belt inherits the pattern of high north and low south of the Jixianian, showing the characteristics of lowering to the south of the basin with the Chua-Yxian area as the uplift centre. The Sinian in the Tianhuan Sag is high in the east and low in the west, and the area of the ZT1 and DC1 wells in the south is relatively high, showing a slope toward the west side of the basin (Fig. 11b).

4.c. Tectonic evolution and transformation process

4.c.1. Tectonic evolution process in the east-west orientation

The east-west tectonic evolution profile of the study area shows that the fault depression layers in the early Changchengian exhibit differential rift sedimentary characteristics controlled by normal

faults. The east and west sides of the Qingcheng-Yulin uplift in the central part of the section develop rift troughs controlled by stepped bidirectional or unidirectional positive faults (Fig. 12a). To the east of the uplift, the secondary active sedimentary filling area corresponding to the end of the Jinshan rift trough on the plane, develops the main rift with approximate bidirectional symmetry and the secondary rift with west-dipping cross-section in turn from west to east, showing a trend of gradually weakening of the magnitude of the rift to the east. On the other hand, in the section west of the uplift, which corresponds to the southwestern depression area on the plane, asymmetric bidirectional faults with the main section tilting eastward and a series of asymmetric bidirectional or unidirectional faults with the main body tilting westward were developed from east to west, which showed a trend of westward subsidence and increase in sedimentary thickness. In the late Changchengian, the extensional rifting and trapping were obviously weakened or tends to be stagnant, and the widely distributed depression layer was developed, and subject to the influence of the rifting and trapping activities in the early stage, the depression layer shows the characteristics of thickening along the profile to the west and thinning to the east (Fig. 12b). This shows that the Changchengian in the study area has experienced the tectonic activities of early rifting and late depression.

The carbonate rocks of the Jixianian are mainly distributed in the area west of the Qincheng-Yulin uplift and show the sedimentary characteristics of the open platform-gently slope that are gradually thickening toward the western trench, revealing the fact that the Jixianian of the western margin of the basin has continued to depress and subside (Fig. 12c). During the Sinian, the main body of the study area was in a state of uplift and denudation, while the tillite was deposited mainly on the western side of the section, with small thickness but still showing a gradual thickening trend toward the western trough, indicating the tectonic characteristics of the western edge of the study area as a result
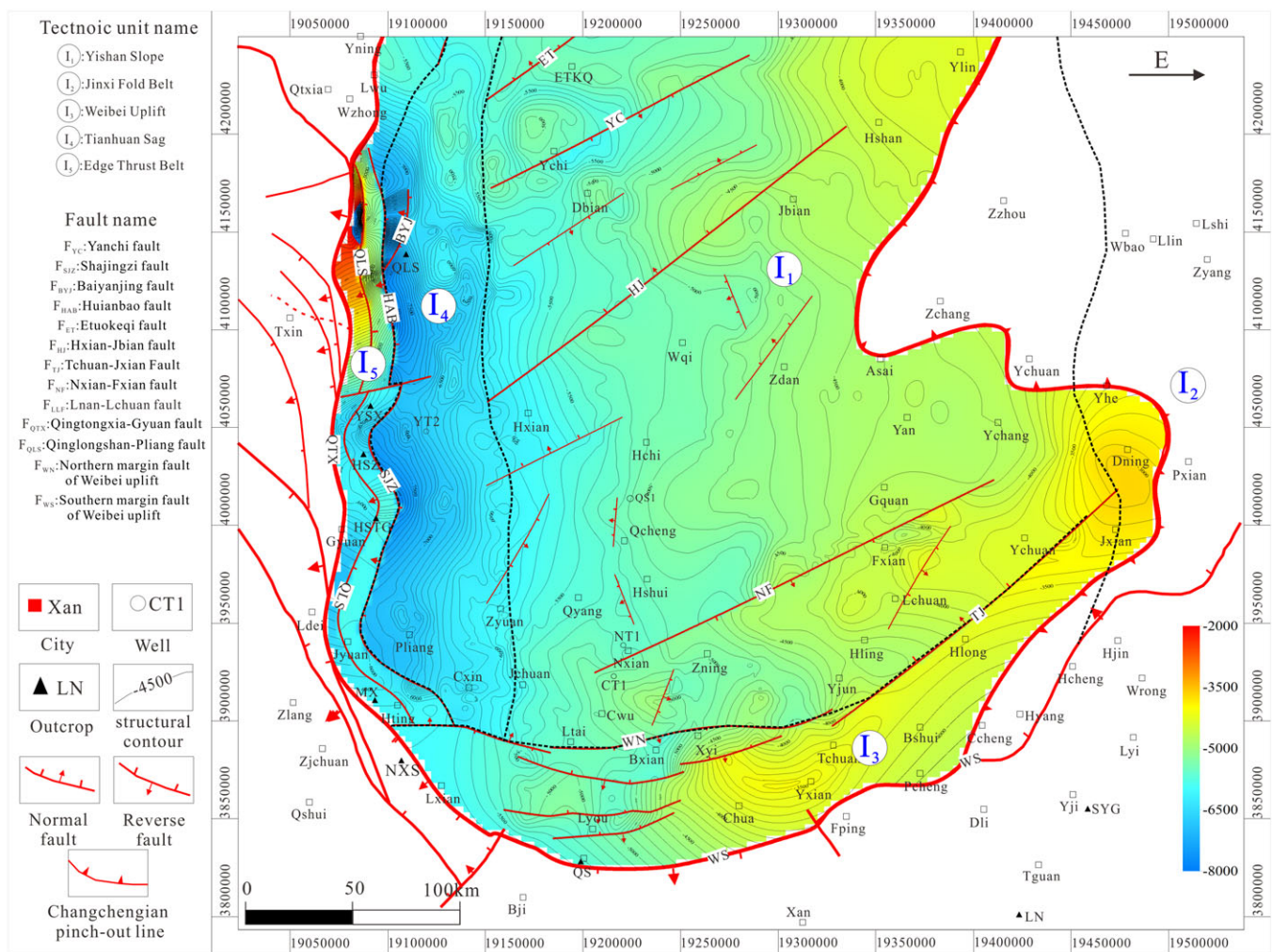
Figure 10. The contour map of the present top surface structure of the Changchengian.

of subsidence (Fig. 12d). Regionally, the Sinian exhibits a parallel or low-angle unconformity contact with both the Jixianian and the overlying Cambrian, indicating that the strata were absent and denuded in the late Mesoproterozoic to Neoproterozoic for more than 800 million years.

In the Early Palaeozoic, the section is separated by a tectonic uplift (Zhenyuan uplift) that lacks the Cambrian-Ordovician system, and there are obvious differences in sediment thicknesses between the east and west sides of the uplift, indicating that the Early Palaeozoic in the study area was dominated by differential uplift and subsidence (Fig. 12e and f). In the Late Palaeozoic, the Permian-Carboniferous, which is thick and widely distributed in the main body of the basin, was developed, revealing the tectonic characteristics of the overall subsidence of the study area in the Late Palaeozoic (Fig. 12g). The reversal of the early normal fault and its associated extrusion deformation on the western side of the Zhenyuan uplift, and the deposition of a more complete Carboniferous system on the eastern side of the uplift in comparison, reveal that the study area was still affected by intra-basin uplift activity in a Proterozoic subsidence context. The regional uplift and denudation of nearly 140 million years from the late Ordovician to the late Carboniferous between the Early and Late Palaeozoic indicates the influence of the Caledonian and Early Hercynian tectonic movements on the internal tectonic evolution of the basin.

The tectonic evolutionary features since the Mesozoic show a distinctly different tectonic pattern from that of the Early Palaeozoic, which was dominated by the western marginal slope, the central plateau marginal uplift, and the eastern intraplateau depression. The thickness distribution of the Triassic system shows a structure of depression in the west and gentle slope in the east (Fig. 12h). The western margin alluvial tectonic activity in the late Jurassic period largely modified the original structure of the Meso-Proterozoic rift and the Early Palaeozoic platform-edge slopes in the study area (Fig. 12i), forming the overall tectonic pattern of the present west-dipping Yishang slope, the low part of the Tianhuan Sag and the Edge thrust belt (Fig. 12j).

4.c.2. Tectonic evolution process in the north-south orientation
The north-south tectonic evolution section shows that the activity of the early Changchengian rift troughs in the study area is different, and the rift troughs on both sides of the Qingcheng-Yulin uplift show different rift assemblages (Fig. 13a). The Jinshan rift trough on the south side of the uplift develops secondary graben-like rifts controlled by stepped normal faults, and the Ganshan rift trough on the north side of the uplift is characterized by the development of opposing secondary faults, and the Changchengian shows a graben-horst composite rift under the clamping of double faults. It shows that the tectonic pattern of
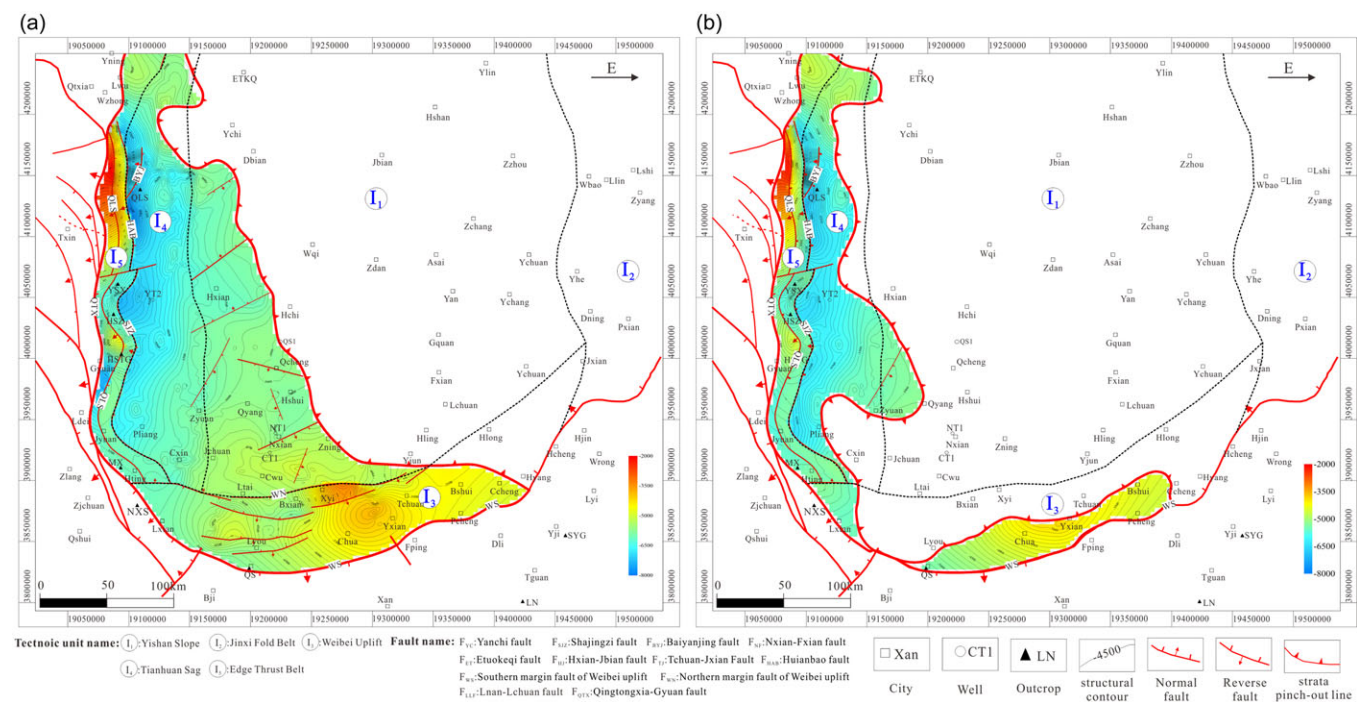
Figure 11. a. The contour map of the present top surface structure of the Jixianian. b. The contour map of the present top surface structure of the Sinian.
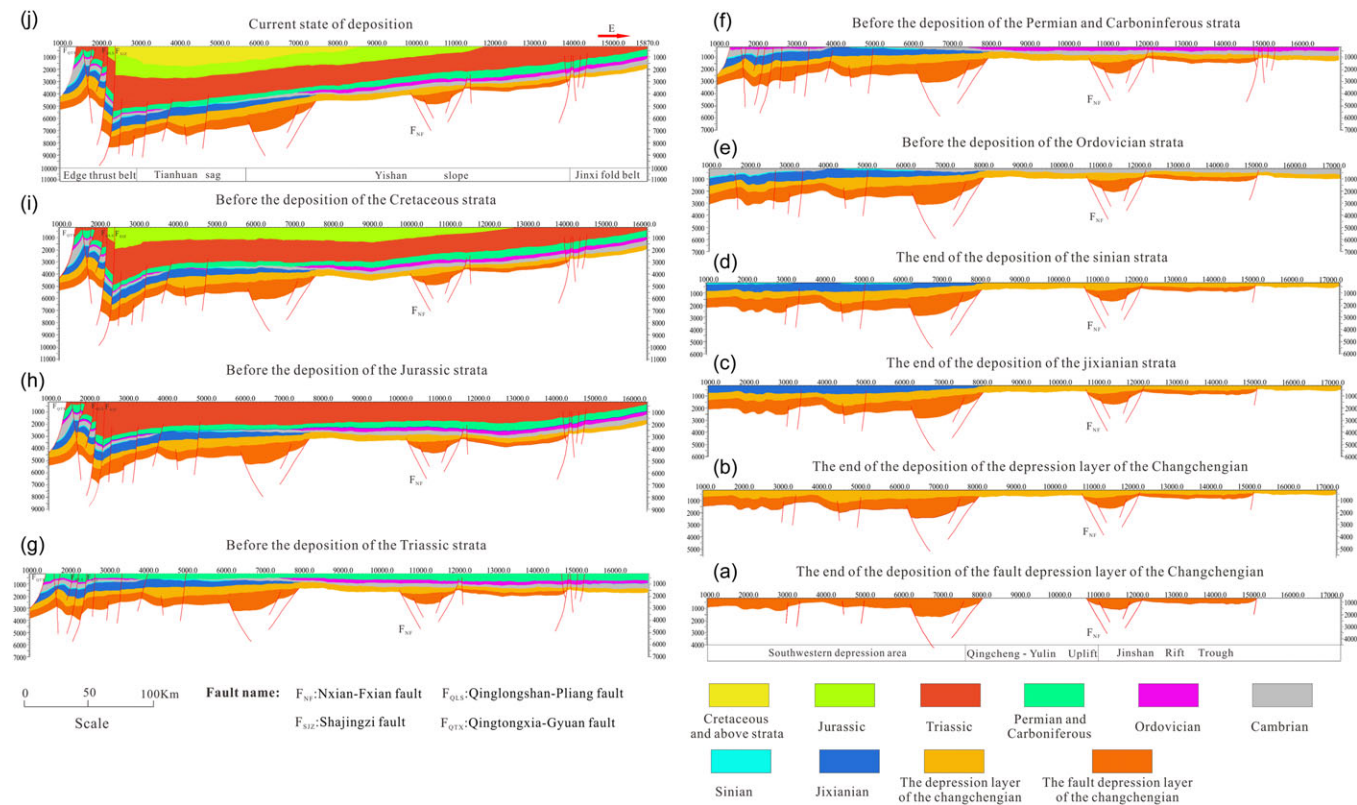
Figure 12. The tectonic evolution history of the east-west orientation in the study area (EWline).

trough and uplift developed in the context of the tensional rift in the early Changchengian. In contrast, during the Late Changchengian, the depression layer was unconformably overlying the fault depression layer and successively thickened in the upper part of the rift trough. This indicates that the extensional rift activity weakened during the Late Changchengian, and the southern part of the basin subsided considerably, expanding the extent of marine intrusion (Fig. 13b).

Figure 13. The tectonic evolution history of the north-south orientation in the study area (NSline).

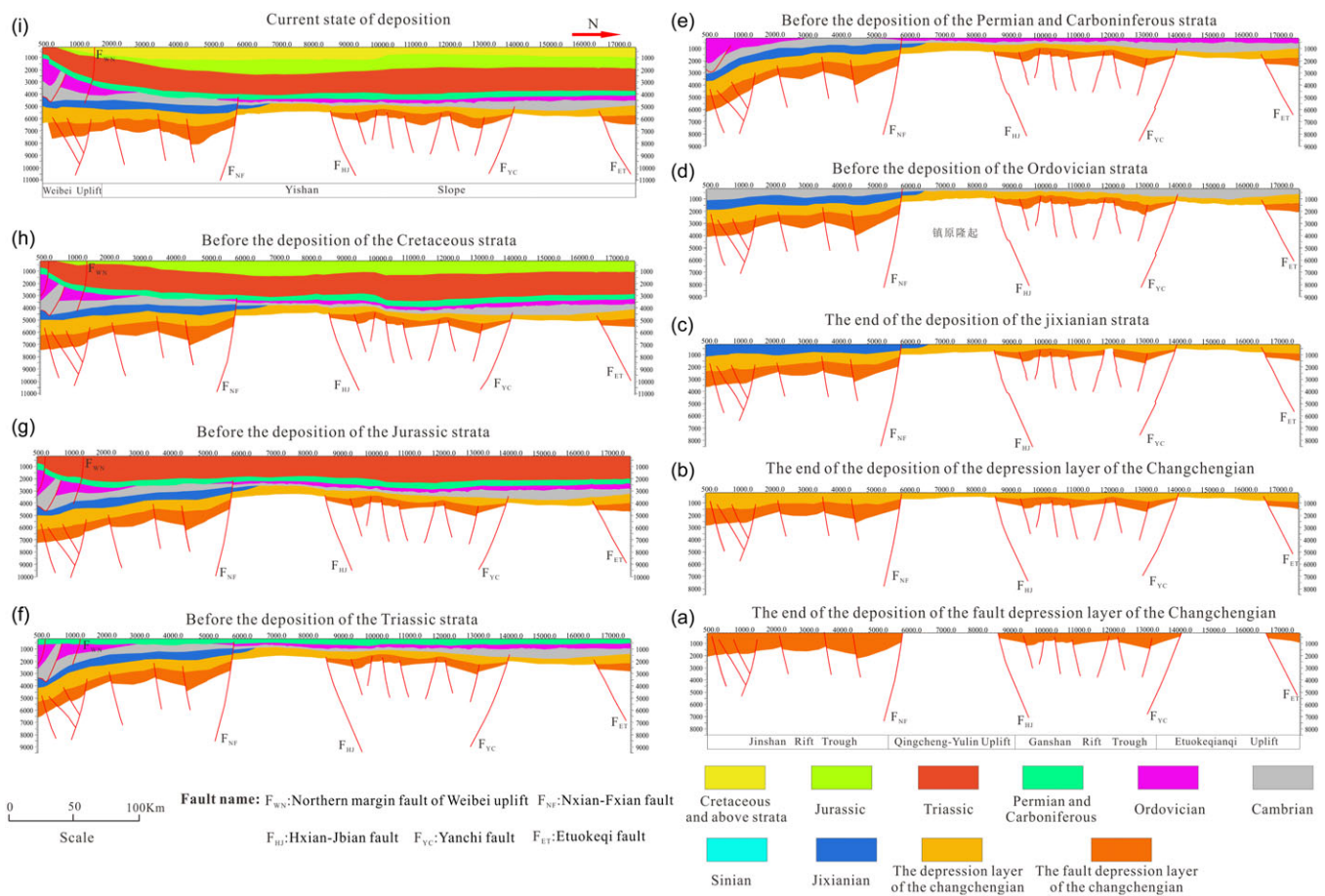The Jixianian thickens south of the Qingcheng-Yulin uplift but is missing north of it. This shows that the central part of the basin uplifted to form the denudation mountain during the Jixianian, while the southern part continued to subside to form a basin-margin slope (Fig. 13c). The overall absence of Sinian in the profile indicates inherited uplift in the central part of the basin, southward expansion of the extent of denuded mountain and small-scale depressional subsidence along the southern margin of the basin (Fig. 13d).

During the Cambrian-Ordovician of the Early Palaeozoic, constrained by the evolution of the North China Plate and the Qilian-Qingling Trough, and in the context of the tectonic stress transition from extension to extrusion, accompanied by the formation of the Central Uplift (Zhi *et al.* 2025), the study area underwent differentiated uplift-subsidence activity. During the Cambrian, under the influence of the subsidence of the passive continental margin in the southern part of the basin and the formation of the central uplift, the sedimentary thickening on the north and south sides of the profile reveals the tectonic pattern of intra-basin uplift and southern depression. In the Ordovician, the continuous uplift of the Zhenyuan made the difference in sediment thickness between the north and south sides more obvious, indicating that the study area underwent an uplift and subsidence process similar to that of the Cambrian (Fig. 13e).

In the Late Palaeozoic, the overall uplift of the basin receives stripping, and the study area deposits thinner Carboniferous and Permian (Fig. 13f). In the Triassic and Jurassic, except for the uplift and thinning of the Weibei uplift area on the south side of the section,

the whole area shows thicker and more stable deposition, indicating the influence of uplift in the southern part of the basin, the relative sedimentation in the basin, and the migration of the sedimentation centre to the inner part of the basin (Fig. 13g and h). The Palaeozoic tectonic landscape has been transformed into the present tectonic pattern of uplift of the southern part of the basin along with the Weibei uplift and subsidence within the basin (Fig. 13i).

4.c.3. Tectonic modification of the Meso-Neoproterozoic

In the early Changchengian, due to the expansion and rifting of the Qinqi and Xingmeng troughs, extensive faulting caused widespread depression along the southern margin of the North China Craton. Along with the continuous extension of the rift on the southwestern margin of the Ordos Basin, the Qin-Qi-He rift system was formed (Wang *et al.*, 2005; Pang *et al.* 2021; Fan *et al.* 2024). As the rift continued to develop and wedge into the study area, two rift troughs emerged: the Ganshan rift trough and the Jinshan rift trough. Meanwhile, uplifts formed on both sides of the rift troughs: the Etuokeqianqi uplift and the Qingcheng-Yulin uplift, establishing the early structural pattern of two troughs and two uplifts. The southwestern margin of the study area, influenced by the expansion and rifting of the Qilian-Qinling trough during the Changchengian, experienced continuous subsidence, resulting in a depression with the thickest Changchengian deposits. This contributed to an ancient topographic feature where the northeast was higher and the southwest lower (Fig. 14a). As rift activity weakened in the middle to late Changchengian, the depression
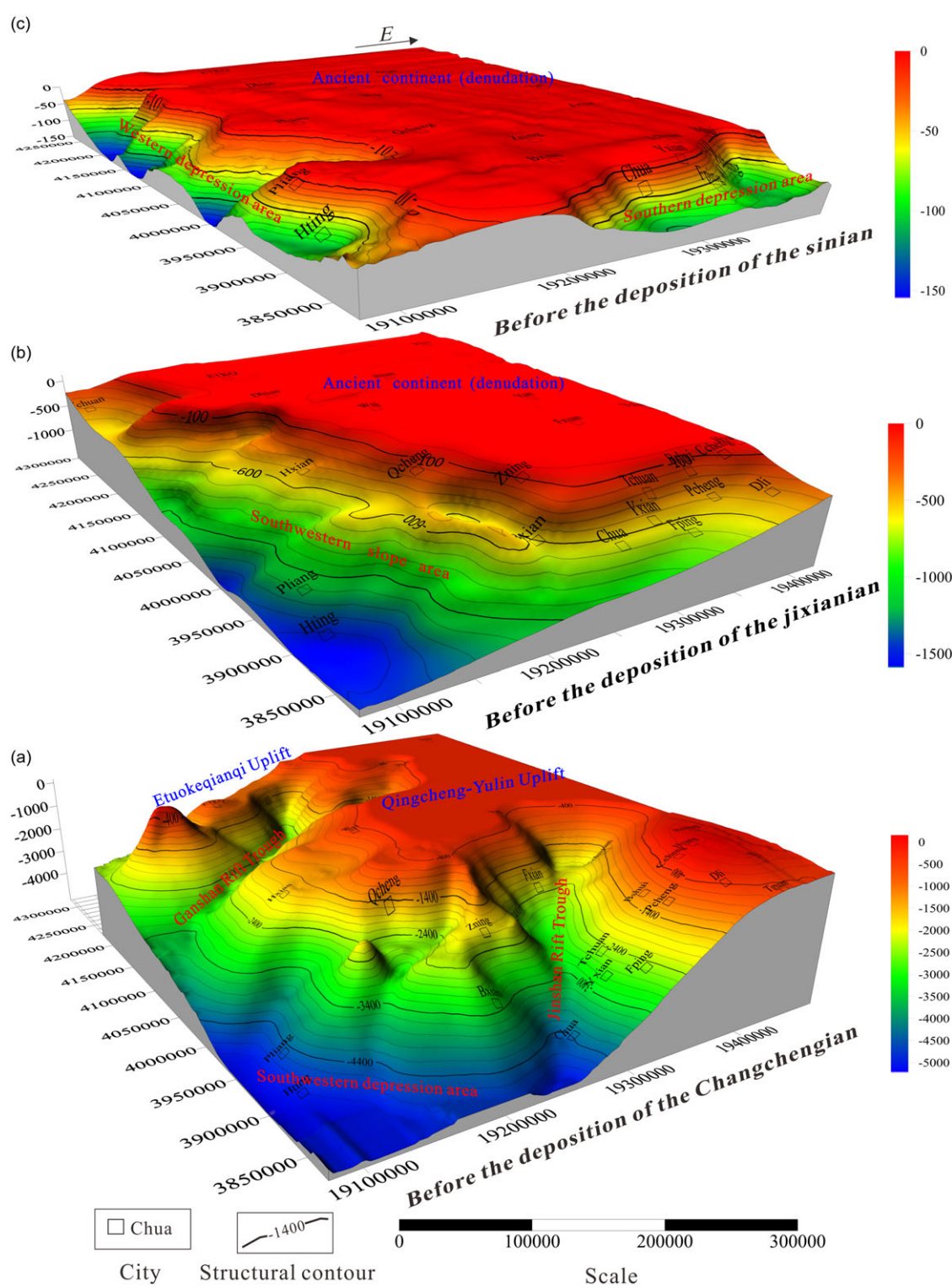
Figure 14. The tectonic modification process of the Meso-Neoproterozoic. a. the ancient structure of the Changchengian. b. the ancient structure of the Jixianian. c. the ancient structure of the Sinian.

layer filled and levelled the ancient topography, causing the sedimentary differentiation between troughs and uplifts in the Jixianian to disappear. Consequently, the central and eastern parts of the study area rose as a whole, while the southwestern part continued to subside based on the pre-existing topographic foundation at the end of the Changchengian, forming a gradually deepening southwestern slope (Fig. 14b). The reduction in the scope of marine transgression during the Jixianian may have also influenced the expansion of the eroded palaeo-land (Gou, 2023; Fan *et al.* 2024; Zhao *et al.* 2024). Notably, the Sinian is largely absent within the basin, being deposited only on the western and southern margins, suggesting that the scope of the eroded palaeo-

land expanded further westward and southward during the Sinian Period. Meanwhile, the main body of the basin formed a high structural area as it rose along with the overall tectonic uplift of the North China Block (Fig. 14c). The active subsidence along the basin margins on the west and south sides potentially represented the reactivation of the basement structures at the basin margins, which laid the foundation for the development of the trough along the southwestern margin of the basin during the Early Palaeozoic (Guo, 2015; Feng *et al.* 2021).

Based on the analysis of two structural evolution profiles, the tectonic process of the Meso-Neoproterozoic in the study area is primarily delineated into four stages: (1) The early rifting and late depression stage of the Changchengian, which served as a pivotal phase in controlling the sedimentary differentiation between troughs and uplifts. (2) The depression stage in the southwestern region during the Jixianian, characterized by a trend towards basin stabilization and a shift towards a tectonic environment dominated by sedimentary activities along the basin margin. (3) The overall uplift and localized subsidence stage in the southwestern margin in the Sinian, during which the sedimentary differentiation in the study area became more evident. The Meso-Neoproterozoic in the northeastern part underwent varying degrees of erosion, while those in the southwestern part accumulated and thickened. (4) The differential uplift and subsidence reworking stage in the Early Palaeozoic, influenced by the uneven uplift-depression differentiation in that period. The Meso-Neoproterozoic underwent a differential reworking process, with uplift in the uplifted areas and depression in the subsidence areas.

5. Discussion

5.a. Significance of structural differentiation to Meso-Neoproterozoic

The 'tectonic differentiation' within a craton basin refers to the differential tectonic deformation produced within the basin under the influence of factors such as changing tectonic stresses or pre-existing structures during different periods, leading to the formation of tectonic units such as rifts, palaeo-uplifts or deep faults within the craton (Wang *et al.* 2017; He *et al.* 2022; Wang *et al.* 2023). The tectonic differentiation in the Ordos Basin is primarily manifested in the changes to the tectonic framework influenced by variations in tectonic stress from the Mesoproterozoic to the Early Palaeozoic, transitioning from rift differentiation in an extensional environment during the Mesoproterozoic to uplift-depression differentiation in a compressive environment during the Early Palaeozoic.

As previously mentioned, under the influence of northwest-southeast tensional stress, the Ganshan rift trough and the Jinshan rift trough developed in the Early Changchengian, with the Etuokeqianqi and Qingcheng-Yulin Uplift existing between the rift troughs. During this period, the basin interior exhibited a rift differentiation pattern of rift troughs and uplifts (Fig. 15a). The development of later fault systems is influenced by early basement faults and regional stress states, while early rift troughs may be reactivated under late extensional settings. This extensional rift environment still influenced the tectonic framework within the basin in the Early Cambrian, as evidenced by the development of northeast-trending rift troughs along the western and southern margins of the basin (Ding *et al.* 2009; Zhang *et al.* 2017). Seismic data reveal that the Cambrian fault system closely aligns with the distribution of basement faults. These basement faults extend

upward to the top of the Cambrian strata, indicating their reactivation during this period. Furthermore, the distribution pattern of Early Cambrian rift troughs corresponds fundamentally with the basement structure reflected by magnetic anomalies. Their spatial consistency with the Changchengian rift troughs demonstrates that the marginal rifts in the Early Cambrian basin represent a differential rifting pattern inherited from pre-existing basement structures. The Late Cambrian to Middle Ordovician period marked a transition in tectonic stress within the basin, shifting from extension to compression (He 2003), with the Middle to Late Ordovician being dominated by a compressive tectonic setting. During and after this period, the basin entered a stage of uplift-depression differentiation (Fig. 15b and c). The Zhenyuan Uplift and the Wushenqi Uplift formed successively. Existing studies on the genesis of uplifts indicate that, although there is debate about the genesis of the Zhenyuan Uplift as the southern high point of the original central uplift of the basin, the cause of eastward compression from the Qilian Trough on the west side of the basin suggests the existence of east-west compressive stress during this period (Zhang, 1997; Zhu *et al.* 2020; Yao 2024). The Wushenqi Uplift is an ancient uplift produced by north-south compressive stress (Mao *et al.* 2023). In addition, the Weibei Uplift in the southern part of the Mesozoic basin formed under the influence of intracontinental compression in the context of the subduction of the ancient Pacific Plate under the Eurasian Plate, roughly synchronous with the regional uplift in the eastern part of the basin during the Cretaceous (Wang *et al.* 2019; Bai, 2020).

These ancient uplifts not only controlled the stratigraphic distribution and sedimentary environments from the Early Palaeozoic onwards but also, to a certain extent, modified the Meso-Neoproterozoic tectonic morphologies under the original rift pattern, forming reworked uplifts of the Meso-Neoproterozoic. As favourable tectonic structural types for hydrocarbon accumulation, the contact relationships between the Meso-Neoproterozoic and the potential hydrocarbon source layers of the Upper Palaeozoic in the uplift areas are complex, which is of great significance for hydrocarbon accumulation in the Meso-Neoproterozoic.

5.b. Two reformed uplifts of the Meso-Neoproterozoic

As two Meso-Neoproterozoic reworked uplifts formed by regional stress changes in the Early Palaeozoic due to tectonic differentiation, the Zhenyuan Uplift and the Wushenqi Uplift exhibit different tectonic characteristics due to differences in their tectonic reworking processes, which in turn control the sedimentary differences in the overlying Palaeozoic strata. The Zhenyuan Uplift is a Meso-Neoproterozoic uplift area in the southwest of the study area, overall presenting an elliptical uplift structure with a steep western wing and a gentle eastern wing (Fig. 16a). The Cambrian-Ordovician formations successively pinch out from old to new around the Meso-Neoproterozoic strata at the core of the uplift, forming a 'Meso-Neoproterozoic window' with missing Lower Palaeozoic strata in the uplift core, which is unconformably covered by the Lower Permian coal measures. The Wushenqi Uplift is located in the Wushenqi-Jingbian area in the north of the study area, with an overall sickle-shaped morphology bent westward. The Changchengian strata at the core of the uplift are exposed, forming a 'window' that is unconformably overlain by the Ordovician strata atop the uplift. In contrast to the Zhenyuan Uplift, the Cambrian formations successively pinch out from new to old around the core of the Wushenqi Uplift (Fig. 16b).
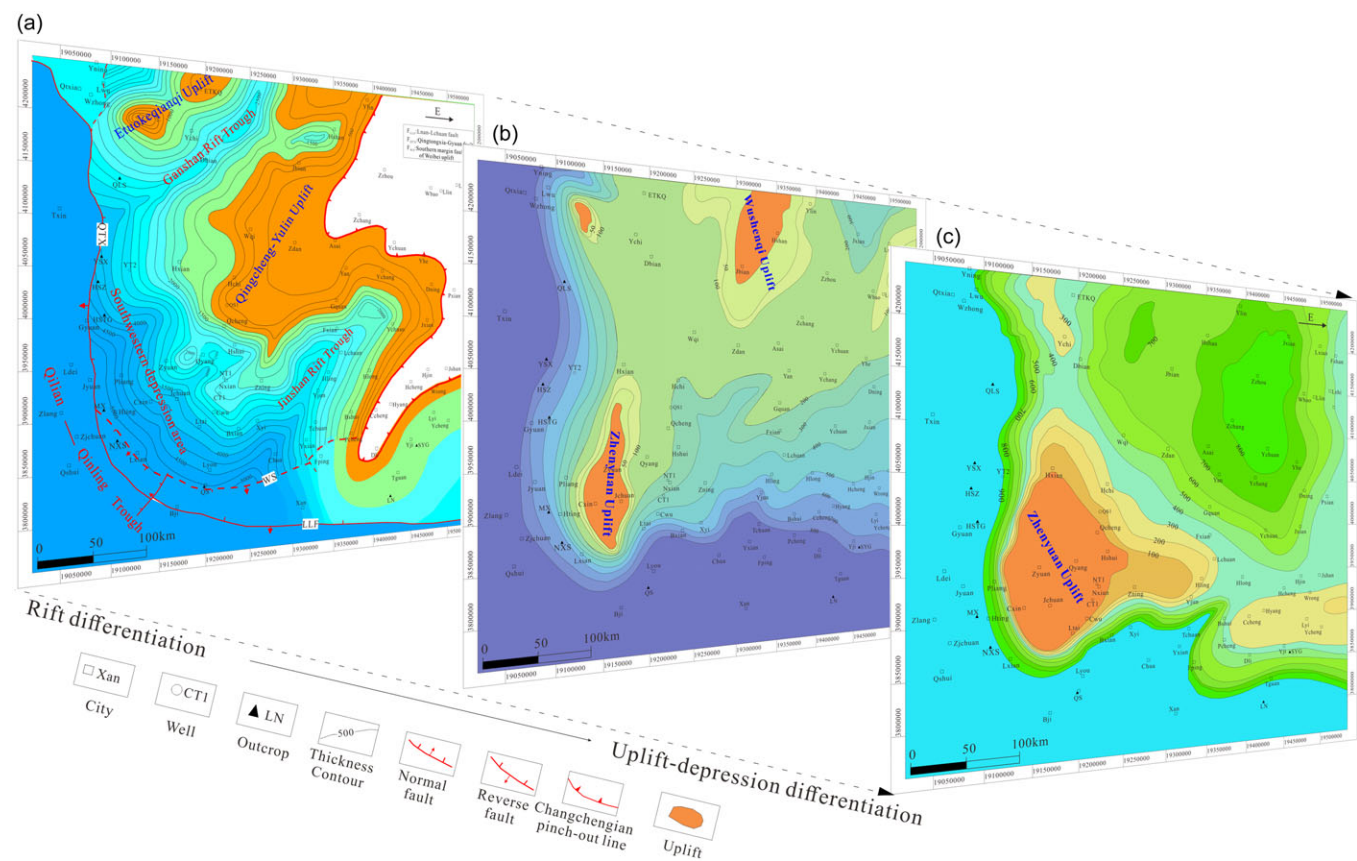
Figure 15. The schematic diagram of tectonic differentiation in the study area. a. the thickness of the Changchengian and the ancient tectonic framework. b. the thickness and ancient tectonic framework of the Cambrian (modified by Ouyang et al. 2023). c. the thickness and ancient tectonic framework of the Ordovician (modified by He et al. 2022).

Based on the analysis of tectonic evolution history, the Zhenyuan uplift underwent four stages: the initial uplift during the Neoproterozoic, continuous uplift during the Early Palaeozoic, subsidence during the Late Palaeozoic and tectonic reversal during the Mesozoic. Prior to Cambrian deposition, the Sinian was thinner on both sides of the uplift and absent in the uplift centre, confirming that differential uplift had already occurred in the late Neoproterozoic. Before the deposition of the Permian-Carboniferous, the Cambrian and Ordovician formations on the slope areas on both sides of the uplift gradually thinned and pinched out towards the uplift core, exposing the Jixianian and Sinian in the uplift core, with the absence of Silurian-Devonian deposits above. This indicates that the Zhenyuan uplift, which had been continuously uplifting during the Early Palaeozoic, remained in an uplifted stage at the end of the Caledonian period. With the overall subsidence of the Late Carboniferous basin, the Carboniferous and Permian formations were unconformably overlying the uplift. During the Mesozoic, the Ordos Basin underwent tectonic uplift in the east and subsidence in the west (2020). The depositional and subsidence centre of the basin gradually migrated westward, causing the Zhenyuan uplift to undergo tectonic reversal and become the subsidence slope area in the west of the basin. This structural-reformation process established a 'window' of the Meso-Neoproterozoic strata at the core of the Zhenyuan uplift, forming a lower-generation and upper-storage assemblage with the overlying Permian-Carboniferous coal-measure source rocks (TOC >30%). Meanwhile, the persistent uplift during the Early Palaeozoic facilitated hydrocarbon migration from Cambrian and Ordovician dolomitic limestones/marls (TOC 0.6–4.5%) on both slopes of the uplift through angular unconformity surfaces. This dual mechanism created a multi-source hydrocarbon charging foundation for gas accumulation in the Zhenyuan uplift.

The Wushenqi uplift developed on the basis of the early Changchengian faulted uplift, undergoing three stages: the Cambrian uplift remnant stage, the Ordovician uplift subsidence stage and the stable burial stage after the Carboniferous (Figure 4–31). The Wushenqi uplift originated by inheriting the terrain of the early Changchengian Qingcheng-Yulin uplift and continued to preserve its uplifted terrain during the Cambrian, resulting in the absence of Cambrian formations in the uplift core. From the uplift core to the slope direction, the Cambrian formations, from younger to older, including the Zhangxia, Xuzhuang and Maozhuang formations, pinched out successively, further confirming that the Wushenqi uplift had already formed before the Cambrian (Wei *et al.* 2021). During the Cambrian, deposition continued on the existing uplifted terrain. After experiencing 'filling and leveling' during the Cambrian and short-term erosion in the early Ordovician, with the expansion of the Ordovician transgression, the uplift area was covered by carbonate rock deposits of the Majiagou Formation. After the Carboniferous, the Wushenqi uplift entered a stage of deep burial, stably receiving the deposition of overlying formations. This structural configuration endows the uplift with a multi-source hydrocarbon charging foundation, comprising Early Palaeozoic source rocks and Changchengian source rocks (dark argillaceous source rocks with
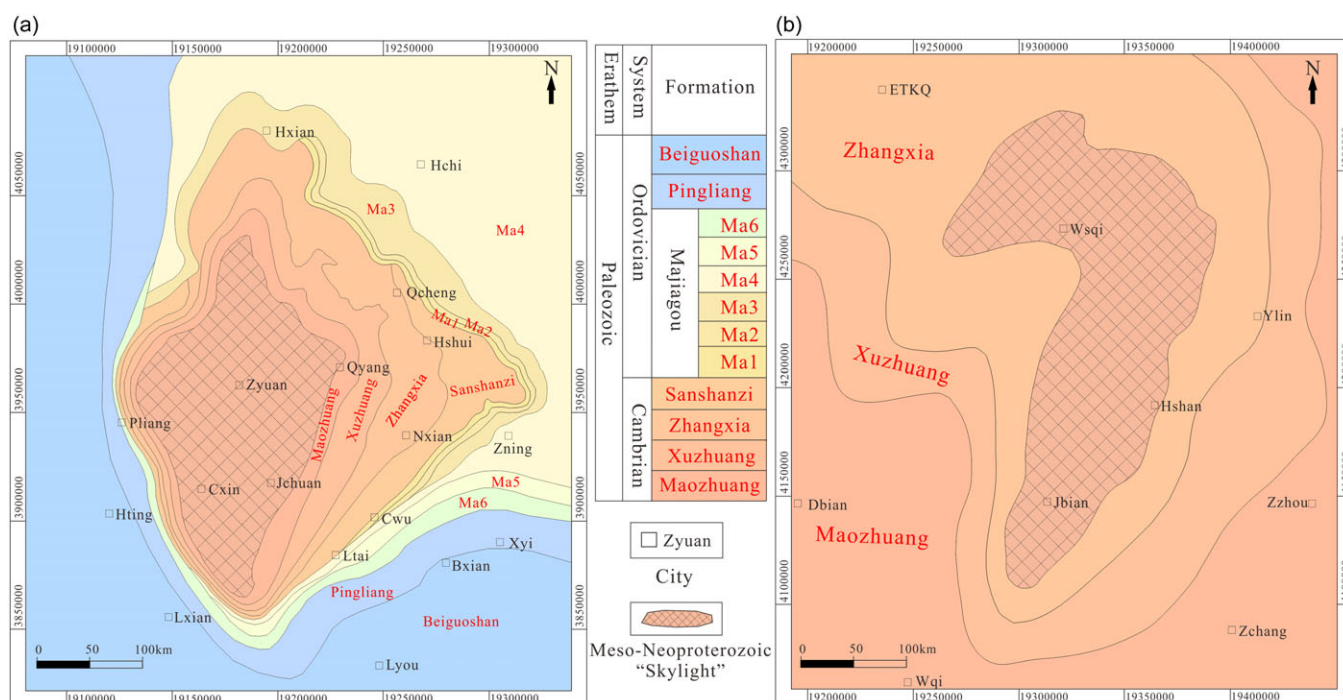
Figure 16. Geological map of the Neoproterozoic uplift in the study area. a. Zhenyuan uplift. b. Wushenqi uplift.

TOC (Total Organic Carbon) >2.3%) within rift troughs along its flanks.

6. Summary and conclusions

The two fault systems in the southern Ordos Basin, namely the basin-margin controlling faults and the intra-basin trough-controlling faults, govern the development and distribution of the Meso-Neoproterozoic formations. From bottom to top, the Meso-Neoproterozoic formations include the fault depressed layer and depression layer of the Changcheng System, as well as the Jixianian and Sinian. The fault depressed layer of the Changchengian exhibits sedimentary characteristics of the NE (Northeast)-trending Ganshan rift trough and Jinshan rift trough, within which two major categories of fault combinations, namely single-fault and double-fault types, are developed in five structural styles: 'graben-like' rift and 'graben-horst' composite rift in the Ganshan rift trough, 'slope-break' and 'fault-block' half-graben-like rift in the Jinshan rift trough, and 'stepped' block-like rift along the southwestern margin.

Through integrated well and seismic interpretation and palaeostructural restoration, the differences in ancient and present tectonic frameworks of the Meso-Neoproterozoic formations have been clarified. During the Changchengian period, the palae-ostructural framework featured a higher east and lower west, with alternating 'two troughs and two uplifts', arranged in a NE-trending oblique pattern from north to south: the Etuokeqianqi Uplift, Ganshan Rift Trough, Qingcheng-Yulin Uplift, and Jinshan Rift Trough. During the Jixianian, the basin sloped southwestward and deepened. In the Sinian, the main body of the basin was denudation palaeocontinent, with depressional subsidence zones along the western and southern margins. In contrast, the present Changchengian exhibits a southwestward-deepening monoclinic structure within the Yishan slope, with the Tianhuan Sag being higher in the north and lower in the south, and the Weibei Uplift

and Edge thrust belt uplifted. The Jixianian shows a higher east and lower west, with higher northern and southern margins and a lower central region. The Sinian presents a modern tectonic framework of higher basin margins and lower basin interior.

The significant differences between the ancient and present tectonic frameworks of the Meso-Neoproterozoic formations are attributed to four tectonic reworking phases: the early rift-late depression sedimentary differentiation stage of the Changchengian period, the basin-margin subsidence stage of the southwestern depression during the Jixianian, the main body uplift and erosion stage of the basin during the Sinian, and the differential uplift and depression during the Early Palaeozoic. Under the influence of tectonic reworking from the Mesoproterozoic rift differentiation to the Early Palaeozoic uplift-depression differentiation, the reworking uplift of the Meso-Neoproterozoic was formed. Both the Zhenyuan Uplift and the Wushenqi Uplift are exposed as 'window' – type uplifts of the Meso-Neoproterozoic formations, formed before the Neoproterozoic and Cambrian, respectively. The Zhenyuan Uplift continued to rise during the Cambrian, while the Wushenqi Uplift maintained its uplifted terrain and was subsequently covered by later Palaeozoic and Ordovician formations after reworking, resulting in a sedimentary pattern with multiple formations in contact with the Meso-Neoproterozoic formations, which is of great significance for hydrocarbon accumulation.

References

Al-Riyami Q, Kelly S and Al-Rawahi A (2005) Precambrian field Oman from Greenfield to EOR. *SPE Reservoir Evaluation and Engineering* **5**, 132–41.

Bai GL (2020) Study on the tectonic evolution of the Weibei uplift in Baoji, Shaanxi. Dissertation, Chang'an University.

Bai HF, Bao HP, Li ZM, Hao SL, Wu CY and Jing XH (2020) Sedimentary characteristics and natural gas potential of the Great Wall System in the Ordos Basin. *Geoscience* **55**, 672–91.

Bai JL, Zhao JF, Ren ZL, Li WH, Wang K and Li X (2022) Paleogeographic and sedimentary evolution of Meso–Neoproterozoic strata in the Ordos Basin, western North China Craton. *Journal of Petroleum Science and Engineering (PA)* **215**, 110600.

Bao HP, Shao DB, Hao SL, Zhang GS, Ruan ZC, Liu G and Ouyang ZJ (2019) Basement structure and early sedimentary cover evolution of the Ordos Basin. *Geological Frontiers* **26**, 33–43.

Cai XF, Yang J, He WK and Zeng ZH (2013) New progress in the study of the Aurignacian System in Helan Mountains–reconceptualization of the Zhengmu Guan Formation and the Rabbit Pit Formation. *Journal of Stratigraphy* **37**, 377–86.

Chen SQ, Zhou YJ, Guo Q, Ruan ZZ, Yu XL and Wang LL (2020) Characteristics and exploration potential of the Mesoproterozoic Aula trough in the Ordos Basin. *Geological Science* **55**, 692–702.

Chen XJ, Hu XJ, Wu Y, Bai YD and Cao YY (2024) Research on the characteristics of the fault system in the middle section of the western margin of Ordos. *Technology Innovation and Application* **14**, 95–8.

Chen YF, Chen JH, Guo B, Li SC, Qi SH, Zhao PP and Li XS (2020) Crustal structure and inter-block deformation relationship in the northern section of the western margin of Ordos. *Chinese Journal of Geophysics* **63**, 886–96.

Cheng CY, He DF and Xu YH (2024) Seismic wave groups and tectonic-stratigraphic sequence characteristics of deep Mesoproterozoic in Ordos Basin. *Chinese Journal of Geology* **59**, 660–72.

Dickas AB (1986) Worldwide distribution of Precambrian hydrocarbon deposits. *Ceoscience Wisconsin* **11**, 8–13.

Ding XQ, Zhang SN, Xie SW and Feng YB (2009) Mesoproterozoic reservoir enrichment pattern in the Mahuangshan area, western margin of the Ordos Basin. *Oil and Gas Geology* **30**, 726–31.

Dong XP (2018) Neoproterozoic sedimentary pattern and geotectonic significance of the western North China Craton. Dissertation, China University of Geosciences.

Efimov AS, Gert AA, Mel'nikov PN, Starosel'tcev VS, Vymyatin AA, Akimov VG, Cherepanova II and Brazhnikova MV (2012) About current sate and trends of hydrocarbon resource potential, geological exploration and licensing in East Siberia and the Sakha Republic (Yakutia). *Geol. Neft. i Gasa* **5**, 57–74.

Fan LY, Qi K, Liu XS, Ren ZL, Li JB, Xing GY, Zhang CL and Cui JP (2024) Degree of thermal evolution of the Middle-Upper Paleozoic-Lower Paleozoic in the Ordos Basin: Indications from the crystallinity of illite and the Yimeng mixing layer. *Geoscience* **59**, 673–82.

Fan YH, Zhu XY, Duan QS, Ma JF, Jia CY, Liu SQ and Zhao TP (2024) Discovery of the 1.79 billion-year-old Yingan porphyry in Taiyue Mountains and its constraints on the genesis of the rift system in the southern North China Craton. *Journal of Petrology* **40**, 1327–42.

Feng JP, Guo YQ and Yu F (2013) Source and sedimentary system analysis of the Yanchang Formation, Fuxian Prospect, Ordos Basin. *Journal of Xi'an University of Science and Technology* **33**, 178–84.

Feng JP, Li WH and Ouyang ZJ (2020) Study on the tectono-sedimentary evolution of the Middle Neoproterozoic in the Ordos area. *Journal of Northwestern University* **50**, 634–43.

Feng JP, Ouyang ZJ and Li WH (2021) Sedimentary characterization of the Middle Proterozoic Jixian system in the Ordos area. *Journal of Northwest University* **51**, 325–32.

Feng JP, Ouyang ZJ, Zhou YJ, Bao HP and Yan T (2018) Redefinition of the "Arcane Trough" in the Middle Proterozoic of the Ordos Region. *Journal of Northwest University* **48**, 587–92.

Gao JP, Zhou LF and Luo TT (2016) Sedimentary characteristics and petrographic paleogeography of the Middle Neoproterozoic in Ordos and neighboring areas. *Groundwater* **38**, 226–28.

Gou JY (2023) Structural and tectonic characteristics of the Middle-Neoproterozoic rift in the Ordos Basin and its genesis mechanism. Dissertation, China University of Geosciences.

Grosjean E, Love G and Stalvies C (2009) Origin of petroleum in the Neoproterozoic–Cambrian South Oman Salt Basin. *Organic Geochemistry* **40**, 87–110.

Guo K (2015) Characterization of Middle and Late Proterozoic Sedimentation at the Western Margin of Ordos Massif. Dissertation, Northwestern University.

Guo YR, Zhao ZY, Zhang YQ, Xu WL, Bao HP, Zhang YL, Gao JR and Song W (2016) Developmental characteristics of marine hydrocarbon system in the Ordos Basin and new areas for exploration. *Journal of Petroleum* **37**, 939–51.

Hao SL, Sun LY, Bao HP, Liu G and Zhang GS (2016) Exploration direction and potential of the Middle-Neoproterozoic in the Ordos Basin. *Natural Gas Geoscience* **27**, 2127–35.

He DF, Bao HP, Gao SL and Li T (2022) Principle of tectonic-sedimentary differentiation and its geological significance. *Journal of Paleogeography* **24**, 920–36.

He DF, Bao HP, Sun FY, Zhang CL, Kai BZ, Xu YH, Cheng X and Zhai YH (2020) Geological structure and genesis mechanism of the Central Palaeouplift in the Ordos Basin. *Geological Sciences* **55**, 627–56.

He ZX (2003) *Evolution and Petroleum Resources of Ordos Basin*. Beijing: Petroleum Industry Press.

Howard JP, Bogolepova OK, Gubanov AP and Gómez PM (2012) The petroleum potential of the Riphean-Vendian succession of south ern East Siberia. Geological Society, London.

Jarrett Amber JM, Cox Grant M, Brocks JJ, Grosjean E, Boreham CJ and Edwards DS (2019) Microbial assemblage and palaeoenvironmental reconstruction of the 1.38 Ga Velkerri Formation, McArthur Basin, northern Australia. *Geobiology* **17**, 360–80.

Jiang ZW and Cai CF (2023) Organic matter accumulation mechanisms and source rock potential of the Mesoproterozoic Xiamaling Formation, Yanliao Basin, North China. *Energy Exploration & Exploitation* **41**, 2016–35.

Kuznetsov VC (1997) Riphean hydrocarbon reservoirs of the Yurulxhen-Tokhom Zone, Lena-Tunguska Province, NE Russia. *Journal of Petroleum Geology* **20**, 459–74.

Li B (2009) Study on the stratigraphy and petrographic paleogeography of the Lower Paleozoic stratigraphy in the Ordos Basin. Dissertation, China University of Geosciences.

Li B (2019) Study on the tectonic and hydrocarbon control factors of the alluvial zone in the western Ordos Basin. Dissertation, Northwest University.

Li M, Yan XB, Zhang W, Guo YL, Liu CY, Fan LL and Yang S (2024) Characteristics and genetic mechanism of the Mesoproterozoic rift system, Ordos Basin, China. *Energy Geoscience* **5**, 1–12.

Li RX, Liang JW and Weng K (2011) Paleoreservoir bitumen of the Jixian system in the southwestern Ordos Basin. *Petroleum Exploration and Development* **38**, 168–73.

Li SZ, Zhang GW, Zhou LH, Zhao GC, Liu X, Xiao YH, Liu B, Jin P and Dai LM (2011) Intra-land differential deformation in the context of Meso-Cenozoic superconvergence: Extensional rifting in North China and extrusion reversal in South China. *Geological Frontiers* **18**, 79–107.

Li XK, Chen G, Zhang FQ, Dang ZH and Liu AJ (2023) Stratigraphic distribution and structural characteristics of the Meso-Neoproterozoic in southern Ordos basin, China. *International Journal of Earth Sciences* **6**, 1853–1869.

Lin CS and Zhang HY (1995) Theoretical basis and new progress of stretching basin simulation. *Geological Frontiers* **3**, 79–88.

Liu G, Yang WJ and Jing XH (2024) Geological characteristics and exploration prospects of the Mesoproterozoic Changchengian in the Ordos Basin. *China Petroleum Exploration* **29**, 44–60.

Liu XG, Zhang J, Yin C, Li S, Liu J, Qian J and Zhao C (2021) Synthetic geochemical and geochronological dataset of the Mesoproterozoic sediments along the southern margin of North China Craton: Unraveling a prolonged peripheral subduction involved in breakup of Supercontinent Columbia. *Precambrian Research* **28**, 3571–6154.

Lottaroli F, Craig J and Thusu B (2009) Neoproterozoic-early Cambrian (infracambrian) hydrocarbon prospectivity of North Africa: A synthesis. *Geological Society, London, Special Publications* **326**, 137–56.

Lu YD (2009) Formation and evolution of the Luonan-Luanchuan fracture zone, East Qinling. *Petroleum Experimental Geology* **31**, 148–53.

Mao DF, He DF, Bao HP, Wei LB, Xu YH, Cheng X, Gou JY and Wu SJ (2023) Distribution, evolution and tectonic properties of the Wutianqi palaeouplift in the Ordos Basin. *Petroleum Exploration and Development* **50**, 755–66.

Mukherjee I and Large RR (2016) Pyrite trace element chemistry of the Velkerri Formation, Roper Group, McArthur Basin: Evidence for atmospheric oxygenation during the Boring Billion. *Precambrian Research* **28**, 113–26.

O'Dell M and Lamers E (2005) Subsurface uncertainty management and development optimization in the Harweel Cluster South Oman. *SPE Reservoir Evaluation and Engineering* **8**, 164–68.

Ouyang ZJ, Feng JP, Ma HY and Li WH (2020) Sedimentary characteristics of the great wall system in the Middle Proterozoic of the Ordos Region. *Journal of Northwestern University* **50**, 105–12.

Pang LY, Zhu XY, Hu GH, Qiu YF, Su WB, Wang SY and Zhao TP (2021) New progress in the study of the Middle-Neoproterozoic age stratigraphic framework and sedimentary evolution process in the southern margin of the North China Craton. *Journal of Stratigraphy* **45**, 180–95.

Peng SQ (2009) Analysis of oil and gas geological characteristics and exploration potential of the Middle and Late Proterozoic in Hangjinqi area. Dissertation, Northwestern University.

Ren SL, Li JH, Li LM, Ge C, Song CZ, Lin SF, Liu GD, Sun WL, Wang JY, Han X and Li ZQ (2016) Study on deformation characteristics and formation environment of Luonan-Luanchuan fault zone (Luanchuan section). *Geoscience* **51**, 1074–89.

Ren ZL, Tian T, Li JB, Wang JP, Cui JP, Li H, Tang JY and Guo K (2014) Progress in the study of thermal evolution history research methods in sedimentary basins and restoration of thermal evolution history in stacked basins. *Journal of Earth Science and Environment* **36**, 1–21.

Sun S, from BL, Li JL (1981) Sedimentary basins of the Middle-Late Proterozoic of Yu-Shan. *Geological Sciences* **4**, 314–22.

Sun ZC and Xie QY (1980) Developmental characteristics of superimposed basins and their hydrocarbon-bearing nature-Taking the Ordos Basin as an example. *Petroleum Experimental Geology* **1**, 13–21.

Tan C, Liu QQ, Wang TS, Li QF and Jia H (2024) Diferential sedimentary evolution of typical aulacogens of Meso-Neoproterozoic in North China craton. *Scientific Reports* **22**, 4410–15.

Wang H, Ren CM, Zhou Z, Wang SJ, Liu YM, Ge MN, Guo TX, Hou QD and Jin JH (2019) Hydrocarbon exploration situation in the Middle-Neoproterozoic of Yanshan area, North China. *Geological Bulletin* **38**, 404–13.

Wang J, Chen PF and Dou QL (2004) Characteristics of hydrocarbon potential in the Middle and Upper Paleozoic of North China. *Petroleum Experimental Geology* **26**, 206–11.

Wang JQ, Liu JY, Yan JP, Zhao HG, Gao F and Liu C (2010) Developmental timeframe and evolution of the Weibei uplift in the southern Ordos Basin. *Journal of Lanzhou University* **46**, 22–9.

Wang SC, Fu ZT, Li XC, Fu JH, Sun FJ and Jiang ZL (2005) Formation and development of the arc tectonic zone of the rift system in the Paleozoic trough-table transition zone at the western margin of the Ordos Basin and its influence on the law of oil and gas aggregation and enrichment. *Natural Gas Geoscience* **4**, 421–27.

Wang SZ, Yang LC and Li ZC (2019) Tectonic features and evolutionary analysis of the Weibei Rise in the Middle-Cenozoic. *Shaanxi Geology* **37**, 58–62.

Wang TG and Han KY (2011) Primary hydrocarbon resources in the Middle Neoproterozoic. *Journal of Petroleum* **32**, 1–7.

Wang YP, Chen LQ, Yang GY, Wu L, Xiao AC, Zhou YJ, Sun LY, Zhang CL, Yang SF and Chen HL (2020) The late Paleoproterozoic to Mesoproterozoic rift system in the Ordos Basin and its tectonic implications: Insight from analyses of Bouguer gravity anomalies. *Precambrian Research*, prepublish:105964.

Wang ZC, Zhao WZ, Hu SY, Xu AN, Jiang QC, Jiang H, Huang SP and Li QF (2017) The controlling role of tectonic differentiation on the formation of large oil and gas fields in the Klatun Basin-An example of the Aurignacian-Triassic in the Sichuan Basin. *Natural Gas Industry* **37**, 9–23.

Wang ZC, Zhao WZ, Huang SP, Zhao RR, Jiang H, Jiang QN, Liu W, Xie WR and Li R (2023) Tectonic differentiation and hydrocarbon enrichment pattern of ancient marine carbonates in the Little Craton, China. *Journal of Geology* **97**, 2842–57.

Wei GQ, Xie ZY, Song JR, Yang W, Wang ZH, Li J, Wang DL, Li ZS and Xie WR (2015) Characteristics and genesis of Aurignacian-Cambrian natural gas in the Sichuan-Chuanzhong ancient uplift, Sichuan Basin. *Petroleum Exploration and Development* **42**, 702–11.

Wei LB, Chen HD, Guo W, Yan T, Cai ZH and Zhou LX (2021) Controls on Ordovician subsalt deposition and reservoirs by the Urumqi-Jingbian palaeorise in the Ordos Basin. *Oil and Gas Geology* **42**, 391–400.

Wu YY, Liu W, Liu Y, Fang X and Ma K (2016) Cambrian subduction deposits in the Gondwana of China and their petroleum geological significance. *Journal of Petroleum* **37**, 1069–79.

Xu YC, Gao Y, Shi YT, Wang Q, Chen AG (2019) Crustal medium anisotropy at the western margin of the Ordos Block: From the Yinchuan graben to the Haiyuan fault zone. *Geophysical Journal* **62**, 4239–58.

Xue G, Lu HF, Zhu CH and Bao HL (2001) Extensional regional equilibrium profiling method and its application in tectonic analysis. *Journal of College Geology* **4**, 427–34.

Yang JJ and Zhang BR (1990) *Basic characteristics of the masked tectonic zone at the western margin of the Ordos Basin. Tectonics and hydrocarbons of the western margin of the Ordos Basin.* Lanzhou: Gansu Science and Technology Press.

Yao JW (2024) Tectonic features and evolution of the central palaeouplift in the Ordos Basin.2024. Dissertation, Changjiang University.

Yusong Y, Yunqin H and Rongqiang Z (2024) Dynamic evaluation on sealing capacity of caprocks of the Meso-Neoproterozoic reservoirs in Ordos Basin, China. Energy Geoscience 5, 132–35.

Zhang CG (2013) Formation and evolution of the Early Palaeozoic central paleorise in the Ordos Basin and the law of material aggregation and distribution. Dissertation, Chengdu University of Technology.

Zhang CL, Gou LL and Di WC (2018) Early Precambrian geological events, nature and geological significance of the western basement in the North China Craton. *Acta Petrologica Sinica* **34**, 981–98.

Zhang CL, Xing FC, Zhang YQ, Jiang FJ, Xu WL and Zhang AM (2023) Tectonic evolution of the Early Palaeoproterozoic Qingyang and Wuqinqi palaeouplift in the Ordos Basin and its control on the palaeogeography of Cambrian lithology. *Oil and Gas Geology* **44**, 89–100.

Zhang CL, Zhang FD, Zhu QY (2017) Rethinking on Cambrian paleotectonics and lithofacies paleogeography of Ordos Cratonic Basin. Oil & Gas *Geology*, **38**(2): 281–91.

Zhang JF, Xiao H, Li MJ, Wang YS, Huang SH, Xu JB and Chen XL (2023) Hydrocarbon sources and formation characteristics of the Middle-Neoproterozoic palaeoproterozoic reservoirs in the Jibei-Liaoxi area. *Journal of Earth Science and Environment* **45**, 42–53.

Zhang JS, He ZX, Fei AQ, Li TB and Huang XN (2008) Large-scale land-edge retrograde thrusting system in the northern section of the western margin of Ordos. *Geoscience* **2**, 251–81.

Zhang QL (1997) Characteristics of plate tectonic genesis and evolution of the Central Palaeouplift in the Ordos Basin and its relationship with the Lower Palaeozoic natural gas accumulation. Dissertation, Nanjing University.

Zhang SH, Li ZX and Evans DAD (2012) Pre-Rodinia supercontinent Nuna shaping up: A global synthesis with new paleomagnetic results from North China. *Earth and Planetary Science Letters*, **13**, 353–54.

Zhang XL (2015) Distribution and depositional environments of the Middle and Upper Proterozoic in the Ordos area and its hydrocarbon exploration potential. Dissertation, Northwestern University.

Zhao CN, Jia S, Xu SY, Lin Y, Xia ML, Lai Y, Zeng YY, Yang J, He KL, Zhu Y, Lu PY, Huang Y and Cheng Y (2023) Determination of the lower limit of porosity in strongly inhomogeneous reservoirs by equivalent substitution method–An example of the Aurignacian Lampshade Formation in Anyue gas field, Sichuan Basin. *China Petroleum Exploration* **28**, 160–66.

Zhao CY (1983) Tectonic evolution of the western margin of the Ordos Massif and analysis of the plate stress mechanism. Inner Mongolia Petroleum Society. Proceedings of the Petroleum Geology of the Western Margin of the Ordos Basin. Hohhot: Inner Mongolia People's Publishing House.

Zhao GJ, Jiang FJ, Zhang Q, Pang H, Zhang SP, Liu XZ and Chen D (2024) Hydrocarbon accumulation process and mode in proterozoic reservoir of Western depression in Liaohe Basin, Northeast China: A case study of the Shuguang Oil Reservoir. *Energies* **17**, 84–92.

Zhao Q, Liu B, Wei LB, Bai HF, Lu FF, Wu C and Shi KB (2024) Characteristics of siliceous endowment and genesis mechanism in dolomites of the Middle Proterozoic Jixian system in the Ordos Basin. *Journal of Geology* **98**, 3117–33.

Zhao WZ, Hu SY, Wang ZC, Zhang SC and Wang TS (2018) Geological conditions and exploration status of oil and gas in the Chinese metapelagic-Cambrian. *Petroleum Exploration and Development* **45**, 1–13.

Zhao ZY, Guo YR, Wang Y and Lin DJ (2012) Progress of tectonic evolution and paleogeographic features in the Ordos Basin. *Special Reservoirs* **19**, 15–20.

Zhi TY, Lv QQ and Liu WW (2025) Characteristics and main controlling factors of Mesoproterozoic-Neoproterozoic carbonate reservoirs in the Ordos Basin. *Fault-Block Oil & Gas Field* **14**, 1–17.

Zhu RJ, Mu MG, Tan ZX, Liu JH and Liu K (2020) Characteristics of tectonic evolution of the central ancient uplift in the southwestern Ordos Basin. *Inner Mongolia Petrochemistry* **46**, 105–06.

Zhu X (1987) On the tectonic evolution of the Chinese continental margin. *Marine Geology and Quaternary Geology* **3**, 115–20.

Zou CC, Du JH, Xu CC, Wang ZH, Zhang BM, Wei GQ, Wang TS, Yao GS, Deng SH, Liu JJ, Zhou H, Xu AN, Yang Z, Jiang H and Gu ZD (2014) Formation and distribution, resource potential and exploration discovery of Aurignacian-Cambrian mega gas fields in the Sichuan Basin. *Petroleum Exploration and Development* **41**, 278–93.